State of the Earth's Cryosphere at the Beginning of the 21st Century: Glaciers, Global Snow Cover, Floating Ice, and Permafrost and Periglacial Environments—

GLOBAL SNOW COVER

By DOROTHY K. HALL, *and* DAVID A. ROBINSON

SATELLITE IMAGE ATLAS OF GLACIERS OF THE WORLD

Edited by RICHARD S. WILLIAMS, JR., *and* JANE G. FERRIGNO

U.S. GEOLOGICAL SURVEY PROFESSIONAL PAPER 1386–A–3

Since April 1960, when the first meteorological satellite image of the Earth was acquired, the remote sensing of snow cover has evolved into a highly quantitative science. Current remote-sensing capabilities enable scientists to measure meter-scale snow cover and snow albedo from space, monitor snowpack ripening, and estimate snow-water equivalent. Hemispheric snow cover can be measured on a daily basis, and snow-cover trends are measured decadally. The 1967–2005 mean annual Northern Hemisphere snow cover extent is 25.6×10^6 km^2. The mean monthly area covered by snow ranges from a January maximum of 46.9×10^6 km^2 to an August minimum of 3.5×10^6 km^2. Snow cover was more extensive during the first two decades of the satellite record than during the more recent decades. Various studies based on satellite data, employing both visible/near-infrared and passive microwave snow maps, show that Northern Hemisphere annual snow-covered area has decreased, mainly because of a decrease in spring snow cover. Since 1988, the mean annual extent is 23.1×10^6 km^2, a statistically significant reduction of approximately 5 percent from the mean annual extent between 1967 and 1986.

CONTENTS

STATE OF THE EARTH'S CRYOSPHERE AT THE BEGINNING OF THE 21ST CENTURY: GLACIERS, GLOBAL SNOW COVER, FLOATING ICE, AND PERMAFROST AND PERIGLACIAL ENVIRONMENTS

GLOBAL SNOW COVER

By Dorothy K. Hall[1] *and* David A. Robinson[2]

Abstract

The first meteorological satellite images of the Earth were acquired in April 1960 from the Television Infrared Observation Satellite-1 (TIROS-1) spacecraft. Those first images revolutionized the study of the Earth from space. Because snow cover has such a high albedo, it was observable on the very first TIROS image, acquired on 1 April 1960, though it was difficult to distinguish the snow from the clouds and even from some other features. Today, more than 50 years later, satellite images reveal unprecedented detail in snow cover. In fact, remote sensing of snow cover has evolved to a highly quantitative science. We now have the capability to measure meter-scale snow cover and snow albedo from space, to monitor snowpack ripening, and to estimate snow-water equivalent (SWE). We can also map hemispheric snow cover on a daily (or more frequent) basis and snow-cover trends decadally. Sensor and image-processing advances have permitted us to map areal extent and quantity of snow cover, with important applications to hydrologic forecasting—including the prediction of flooding and water supply. National Oceanic and Atmospheric Administration (NOAA) maps of snow extent, from 1966 to the present, combined with more recent Moderate Resolution Imaging Spectroradiometer (MODIS)-derived maps of snow cover and albedo and with passive-microwave-derived maps of snow extent and SWE, are available for development of quality-controlled, decade-scale records called climate-data records (CDRs). CDRs will provide detailed, quantitative information to modelers and will permit climatologists to model and monitor snow-cover trends for decades into the past and future. Active-microwave instruments, such as scatterometers and synthetic-aperture radars (SARs), can yield information about snowpack ripening, snow depth, and SWE. Still, many uncertainties remain, and validation of remotely sensed measurements against ground observations and measurements will continue to be necessary, especially in complex terrain. An ongoing activity is refining the errors in the remotely sensed measurements and focusing on developing new sensor technologies capable of characterizing snow volume in mountainous areas and vegetated land covers.

Introduction

The mean geographical extent of snow cover in the Northern Hemisphere varies from a maximum of 46.9×10^6 km^2 in January and February to a minimum of 3.5×10^6 km^2 in August; 60 to 65 percent of winter snow cover is in Eurasia, and most midsummer snow cover overlies the high-elevation regions of the Greenland ice sheet (Robinson and others, 1993; Frei and Robinson, 1999). In the Southern Hemisphere, most of the seasonal snow cover is in South America, where the extent of snow cover has been reported to reach

[1] Cryospheric Sciences Laboratory, Code 615, NASA/Goddard Space Flight Center, Greenbelt, MD 20771, *dorothy.k.hall@nasa.gov*

[2] Global Snow Lab, Department of Geography, Rutgers University, Piscataway, NJ 08854, *drobins@rci.rutgers.edu*

1×10^6 km^2 (Dewey and Heim, 1983), although measurements using advanced sensors in more recent years show a lower snow extent than that, as discussed later. Except on the Antarctic Peninsula and in coastal regions, very little snowmelt occurs in Antarctica, where only about 2 percent of the continent is bedrock exposed during part of the year.

The need to quantify snow cover, and especially snow-water content, is ever increasing. As much as 80 percent of the water supply in the western United States is derived from snowmelt, and many countries—especially those that are dominated by mountainous terrain—rely on snowmelt for water supply and generation of hydropower. Melting snow in the Himalayan region, for example, becomes runoff to rivers that supply water to more than one-half billion people. The total amount of snow and the rapidity of snowmelt are important factors governing spring flood potential and summer drought.

Snowmelt forecasting is used to predict floods and snowmelt runoff in alpine-dominated regions of the world. Mountain snowfields act as natural reservoirs for water-supply systems, storing precipitation in the form of snow and then releasing water into streams and rivers as the snow melts. In recent decades, improvements in technology have contributed to advances in the measurement of snow cover on local to global scales.

One of the striking characteristics of snow cover is its very high albedo, which aids the mapping of snow cover from aircraft- and satellite-derived data from the visible and near-infrared parts of the electromagnetic spectrum. Global-scale, satellite-derived maps of snow cover have been generated by use of a variety of satellites, sensors, and algorithms. Snow-cover mapping can be accomplished at a variety of temporal and spatial scales with unprecedented accuracy. Snow maps can be produced by means of data from the visible, near-infrared, and microwave parts of the spectrum, allowing different snowpack characteristics to be studied.

Modeling contributes to a better understanding of the variability of snow cover on annual to decadal scales, of cryosphere-climate interactions, and of the role snow may play in regional and global climate change. Forecasting of local daily temperatures, regional climatic anomalies, and location and strength of cyclonic systems with increasing accuracy relies on knowledge of the distribution and state of regional snow cover; thus, highly accurate snow-extent data are required as input to models. Models also simulate the influence of regional and global climate on snow cover and, conversely, the impact of snow cover on climate.

The presence of snow cover has an important influence on climate, mainly because of the strong positive feedback of spring snow cover on the radiation balance over the Northern Hemisphere (Groisman and others, 1994; see also, for example, Kukla (1981), Foster and others (1983), Walsh (1984), and Barnett and others (1989)). Recent evidence suggests that reductions in snow cover over large parts of the Arctic have contributed to Northern Hemisphere [climate] warming (Stone and others, 2002). Earlier studies (Foster, 1989; Foster and others, 1992) found that the date on which the tundra became snow free in Barrow, Alaska, had occurred progressively earlier since the 1940s.

Understanding the influence of interannual variability in snow cover on climate is facilitated by hydrologic models. Models show, for example, that extensive winter/spring Eurasian snow cover is linked to weak rainfall in the following summer Indian monsoon season (Barnett and others, 1989; Vernekar and others, 1995). Extensive snow cover in Eurasia in February

reduces summer precipitation over India because the energy used in melting snow reduces the surface temperature over a broad region centered on the Tibetan Plateau.

Early season snow-cover variability leads to altered general circulation patterns consistent with the dominant mode of winter variability observed in the Northern Hemisphere troposphere (Cohen and Entekhabi, 1999). Furthermore, there is a relationship between changes in the strength of the winter North Atlantic Oscillation and the Arctic Oscillation and the variability and timing of snow cover in Europe and the North Atlantic (Schaefer and others, 2004).

In the following paragraphs in this section, we give a brief description of the relationship between snow and climate and a history of seasonal snow-cover mapping, with a focus on the continental and global scales. We then review available products and observations of changes in snow-cover extent. Finally, we examine the current and future status of seasonal snow-cover mapping, including the development of a climate-data record (CDR) of snow cover.

Brief History of Snow Mapping

The first recorded snow surveys took place in 1834 in the State of New York, yielding a report on the areal extent and water content of a snowpack on the watershed of Madison Brook, N.Y. (Santeford, 1974). In 1906, the U.S. Weather Bureau sponsored monthly snow surveys near Lake Tahoe, Nevada, by Dr. James E. Church, a professor of classics from the University of Nevada. Soon thereafter (1908–09), Dr. Church led the development of the Mt. Rose Snow Sampler, the world's first snow surveying equipment to measure snowpack water content (Stafford, 1959); a variation of this sampler is still in use today. Other western states, notably Utah and California, soon began conducting snow surveys with the Mt. Rose Snow Sampler.

Ground-based photographs have long been used to map the areal extent of snow cover (Potts, 1937). By 1953, the California Electric Power Company had established a program to measure snow depth from aircraft in the Sierra Nevada Mountains for water-supply forecasting (Stafford, 1959). Other observations, made from aircraft, are used in mapping snow cover and delineating the snowline.

A major step forward in snow mapping came with the advent of satellites (Singer and Popham, 1963). Because of its high albedo, snow was easily observed even in the first images obtained from the Television Infrared Operational Satellite-1 (TIROS-1) meteorological satellite on 1 April 1960. Before the satellite era, there were attempts to map snow cover globally by means of station observations and aerial photographs (for example, Rikhter, 1960; Mellor, 1964), but it was not possible to view snow cover all over the world at the same time, or to differentiate snow from most clouds on imagery, or to do detailed snow mapping. In the mid to late 1960s, satellite sensors began to transmit snow-cover images that permitted operational snow-cover mapping (fig. 1). Today, satellite-borne instruments yield detailed information on snow cover in the visible, infrared, and microwave parts of the electromagnetic spectrum on a daily basis.

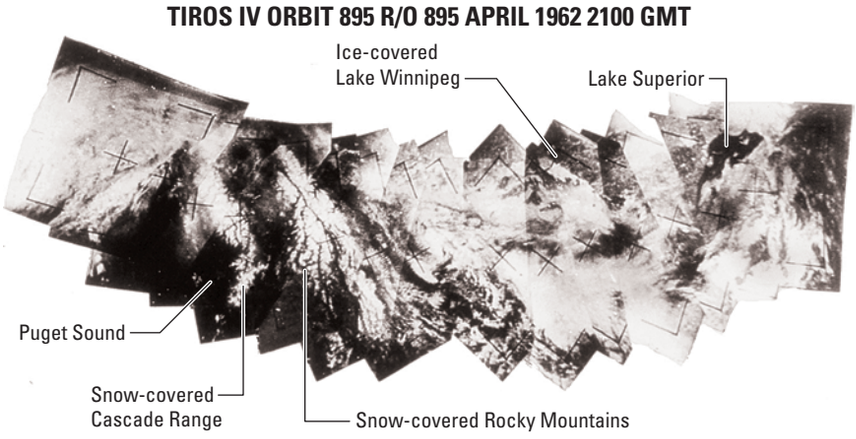

Figure 1.—*Images acquired on 11 April 1962 from the Television Infrared Observing Satellite-4 (TIROS-4), taken from an altitude of about 700 km. Clouds and snow are indistinguishable in parts of the image mosaic.*

Satellite-Based Snow Detection

Snow Mapping in the Reflective Part of the Electromagnetic Spectrum

The Earth Resources Technology Satellite-1 (ERTS-1), later renamed Landsat-1, was launched on 23 July 1972; it carried Multispectral Scanner (MSS) and return beam vidicon (RBV) sensors with a picture element (pixel) resolution of 80 m. The Landsat-1 satellite was the first in a series of six satellites that have been launched successfully over a period of nearly 30 years. Landsats-2 and -3 were launched on 22 January 1975 and 5 March 1978, respectively, also carrying MSS and RBV instruments; Landsat-3, however, carried an improved RBV sensor with a pixel resolution of 30 m. Landsats-4 and -5, launched on 16 July 1982 and 1 March 1984, respectively, carried a Thematic Mapper (TM) with 30-m pixel resolution (as well as an MSS sensor), providing even greater detail for snow-cover mapping than did the MSS. The Landsat-6 satellite, launched on 5 October 1993, failed to achieve orbit. Landsat-7 was launched on 15 April 1999 with the Enhanced Thematic Mapper Plus (ETM+) instrument on board, representing another advance in the Landsat series instrument technology. Only Landsats-5 and -7 are still operating at this writing (March 2008), and a failure of the scan-line corrector (SLC) on 31 May 2003 has greatly diminished the utility of data from the Landsat-7 ETM+.

With the advent of Landsat data came the ability to create detailed basin-scale snow-cover maps on a regular basis, barring cloud cover (Rango and others, 1977). Furthermore, Landsat images were used to demonstrate the utility of developing snow-cover depletion curves used in hydrologic modeling for streamflow estimation, though there are substantial limitations to the use of Landsat data for snow-cover mapping. For example, the Landsats-1 through -5 MSS and TM sensors were not designed to provide detail of high-reflectance surfaces, such as snow; therefore, the sensors saturated in the visible parts of the spectrum over some snow-covered areas, a problem well known to glaciologists (Ferrigno and Williams, 1983). The ETM+ has two gain settings to optimize the sensor sensitivity. In the low-gain mode, the sensors do not saturate over snow because of the greater dynamic range. Though the Landsat series

(fig. 2) has provided high-quality, scene-based snow maps, the 18- or 16-day repeat-pass interval of the Landsats-1 through -3 and Landsats -4, -5 and -7, respectively, is not adequate for most snow-mapping requirements, especially to capture the rapid changes during the spring snowmelt period. Despite the limitations, early Landsat data were pivotal for snow-mapping studies because the algorithms used to develop snow maps (for example, Dozier, 1989) became the heritage algorithms for subsequent regional and global products; experimentation with spectral bands on the Landsat sensors led to optimum band selections on subsequent sensors. Furthermore, advanced regional mapping techniques such as spectral unmixing (Nolin and others, 1993; Rosenthal and Dozier, 1996) have been developed and tested with Landsat data.

Since 1966, data from geostationary operational environmental satellites (GOES) and data from the Very High Resolution Radiometer (VHRR) and its successor, the Advanced Very High Resolution Radiometer (AVHRR), on polar orbiting environmental satellites have been used extensively by the National Oceanic and Atmospheric Administration (NOAA) to produce operational snow products (Matson and others, 1986; Carroll, 1995; Ramsay, 1998). Trained meteorologists map snow-cover extent from visual analyses of visible satellite imagery. Snow-cover identification is made by manual inspection of hardcopy imagery and graphics products, online imagery loops, and the previous day's and (or) week's analysis. Map quality is predicated on the availability of clear-sky visible imagery and the meteorologist's experience.

Since 24 February 2000, the Moderate Resolution Imaging Spectroradiometer (MODIS) instrument has been providing daily snow maps at a variety of temporal and spatial resolutions (Hall and others, 2002; Hall and Riggs, 2007). MODIS is a 36-channel spectroradiometer that was first launched as part of the National Aeronautics and Space Administration (NASA) Earth Observing System (EOS) program on 18 December 1999 on the Terra spacecraft. A second MODIS was launched on 4 May 2002 on the Aqua spacecraft. The sensors on the MODIS instrument provide a large suite of land, atmosphere, and ocean products, including daily maps of global snow-cover (fig. 3) and sea ice (Hall and others, 2004). Snow-cover maps, developed from the NOAA and MODIS sensors, are discussed later in more detail.

Snow Albedo

Albedo is a key global energy-balance parameter that determines how much solar energy is absorbed by the Earth's land (or water) surface. Biogeochemical, ecological, and hydrologic processes are influenced strongly by the amount of available solar energy. The albedo of fresh snow can be 85 percent or more, but it drops to less than 50 percent as snow ages and melts. Snow albedo depends on many factors, including grain size and shape, snow stratigraphy, surface roughness, liquid-water content, impurities, depth, and the surface beneath the snowpack.

The deposition of snow cover can drastically alter the local energy balance because the albedo of non-snow-covered land is generally much lower than that of snow-covered land. As a snowpack metamorphoses, albedo can decrease by more than 25 percent within just a few days as growth of snow grains proceeds (Nolin and Liang, 2000), especially if the snowpack becomes wet. The albedo of snow cover is also highly dependent on the land surface, that is, whether the snow falls on a forest or over the tundra, to cite two

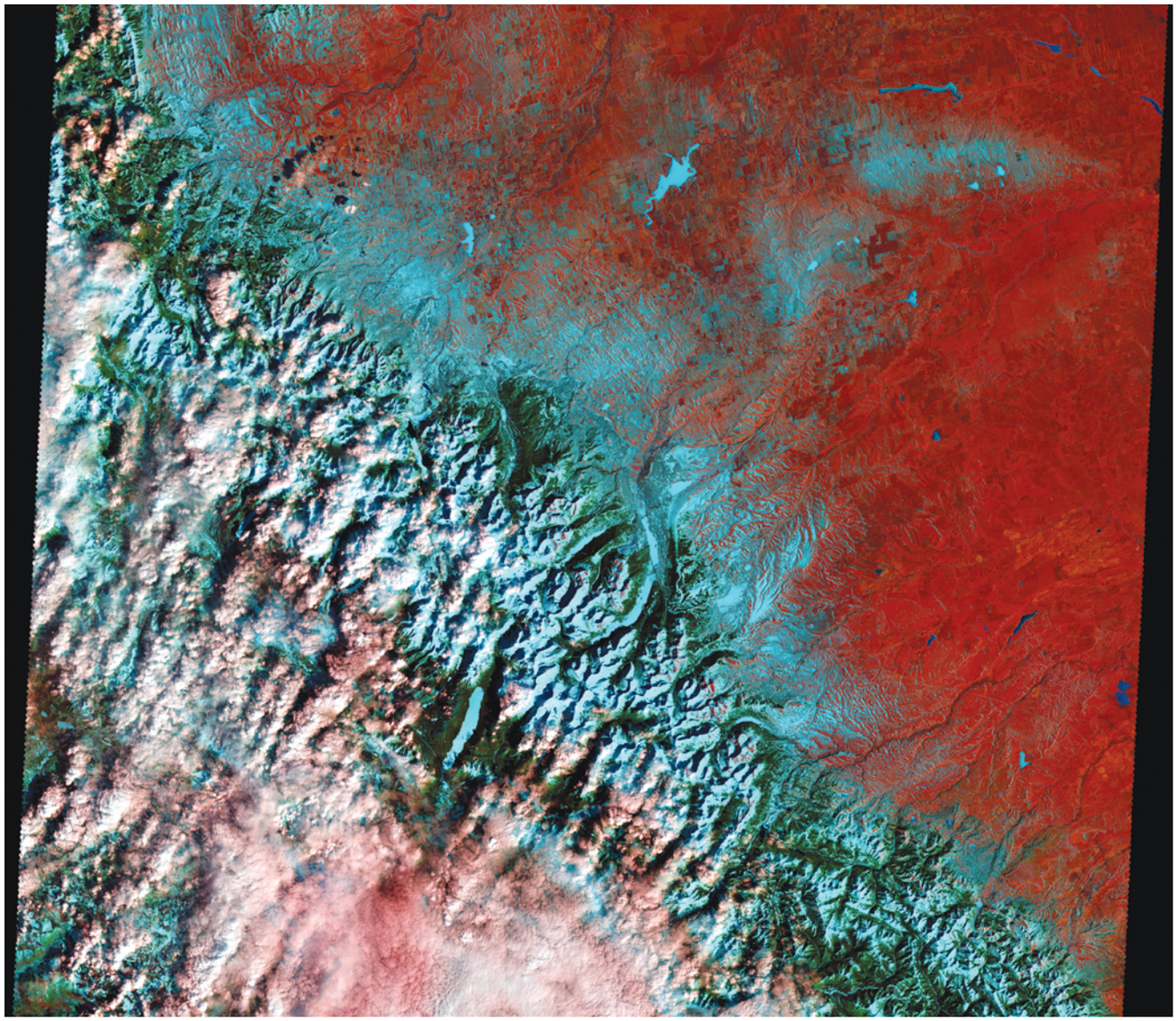

Figure 2.—*Landsat-5 Thematic Mapper (TM) image of Glacier National Park, Montana, acquired on 14 March 1991, showing snow-covered mountains. Clouds obscure parts of the lower part of the image and appear as white or pink, whereas snow cover (including snow-and-ice-covered lakes) is blue and non-snow-covered, vegetated land is reddish orange. Landsat 5 TM false-color composite image 2569–17454, Path 69, Row 17, from USGS EROS Data Center, Sioux Falls, S. Dak.*

extremes. For low vegetation, the depth of the snow cover has a major influence on the scene albedo; once the snow gets deep enough to cover the vegetation, then albedo can be much higher.

Many early remote-sensing studies of snow albedo were done from aircraft (for example, see Bauer and Dutton, 1962; McFadden and Ragotzkie, 1967; Salomonson and Marlatt, 1968; Dirmhirn and Eaton, 1975). Later, using satellite data, some researchers measured the albedo of snow-covered lands by constructing basinwide albedo maps (Kukla and Robinson, 1980; Robinson and others, 1986; Scharfen and others, 1987). Robinson and Kukla (1985) used Defense Meteorological Satellite Program (DMSP) imagery (spectral

Figure 3.—*A 500-m-pixel-resolution Moderate Resolution Imaging Spectroradiometer (MODIS) image of New Zealand's South Island, acquired on 11 July 2003. The intense storm that produced this snow cover was reported to be the worst blizzard to hit the country in 50 years. Image courtesy of NASA's MODIS Land Rapid Response Team.*

range, 0.4–1.1 μm) to derive a linear relationship between the brightest snow-covered arctic tundra and the darkest snow-covered forest, which were assigned albedos of 0.80 and 0.18, respectively. Scene brightness, a function of the type and density of vegetation and the depth and age of snow (Robinson and Kukla, 1985), was then converted to surface albedo by linear interpolation.

Detailed field, aircraft, and satellite studies have been used to derive quantitative measurements of snow reflectance and albedo (for example, see Robock, 1980; Dozier and others, 1981; Steffen, 1987; Hall and others, 1989; Duguay and LeDrew, 1992; Winther and others, 1999; Greuell and others, 2002; Klein and Stroeve, 2002; Stroeve and others, 2005). Surface albedo may be derived from Landsat TM and ETM+ data. One approach, based on exact solutions of the radiative-transfer equation for upwelling intensity, requires known albedo values derived in each Landsat scene at various points (Mekler and Joseph, 1983). Other approaches rely on a narrowband to broadband conversion to derive albedo. Knap and others (1998) used Landsat data to derive the Bi-directional Reflectance Distribution Function (BRDF) to describe the complete distribution of the anisotropic reflectance of snow.

NOAA National Environmental Satellite, Data, and Information Service (NESDIS) Snow Maps

NOAA's National Environmental Satellite, Data, and Information Service (NESDIS) started to generate operational Northern Hemisphere Weekly Snow and Ice Cover analysis charts in November 1966 using manual techniques from NOAA satellite data, at a nominal pixel resolution of 190 km. After all snow boundaries were identified and placed on a hardcopy polar stereographic projection map, an electronic version was made through the digitization of a 89×89 cell acetate overlay (mid- and high-latitude portion of a hemispheric 128×128 cell overlay) (fig. 4). Through the years, improvements in snow mapping have resulted from improved sensor resolution and use of more consistent mapping techniques. The NOAA/NESDIS snow maps are the premier dataset used to evaluate large-scale snow extent of the Northern Hemisphere (Matson and others, 1986; Robinson and others, 1993; [*http://climate.rutgers.edu/snowcover/*]). To date, these maps constitute the longest satellite-derived environmental dataset available. Early NOAA/NESDIS snow maps (pre-1972) tend to underestimate snow-cover extent, particularly during the fall (Kukla and Robinson, 1981). A major reason for this problem was the inexperience of early analysts in distinguishing snow cover from clouds or even from snow-free ground, compounded by the lower pixel resolution of imagery during this era (pre-1972) compared to the period since. Because of the difficulties with the pre-1972 NOAA/NESDIS maps, the Rutgers Global Snow Lab (GSL) reanalyzed snow cover between 1966 and 1971 using the same NOAA daily gridded composites of visible imagery for the eastern and western hemispheres of the Northern Hemisphere used in the original mapping. Surface resolution of the revised imagery is approximately 25 km. The imagery was supplemented with daily reports of snow depth at several thousand stations in the United States, Canada, China, and the Former Soviet Union, gridded to 1°×1° grid cells using all reports from within a given cell. Daily surface weather charts also provided information on cloud cover, precipitation, and temperature. Infrared imagery and the above ancillary information were employed in many areas to validate interpretations made from visible data.

In 1997, the Interactive Multisensor Snow and Ice Mapping System (IMS) [*http://www.ssd.noaa.gov/PS/SNOW/ims.html*] was instituted to produce operational products daily at a spatial resolution of about 25 km, based on a variety of satellite data (Ramsay, 1998). Improvements in the spatial resolution of the IMS product in February 2004 resulted in improved snow maps at 4-km resolution (fig. 4). In June 1999, NOAA/NESDIS ceased producing the weekly maps, replacing them with the daily IMS product (Ramsay, 1998). IMS maps are generated from a UNIX-based workstation application that allows the analyst to visually inspect imagery and mapped data from various sources to determine the presence of snow. Daily maps are produced from a variety of visible satellite imagery, estimates of snow extent derived from microwave satellite data, and station-mapped products. Maps were digitized to a 1024×1024-cell polar grid through January 2004; a 2048×2048-cell polar grid is used at present. Since 2000, the IMS snow-cover maps have been produced by NOAA's National Ice Center in Suitland, Maryland.

Before the weekly map series ended in 1999, there was a 2-year period in which the weekly NOAA/NESDIS map and the daily IMS map were both produced. Data from this interval are being analyzed at Rutgers to develop an accurate means of converting the daily maps to a weekly product at the lower resolution so that the long-term record can be continued.

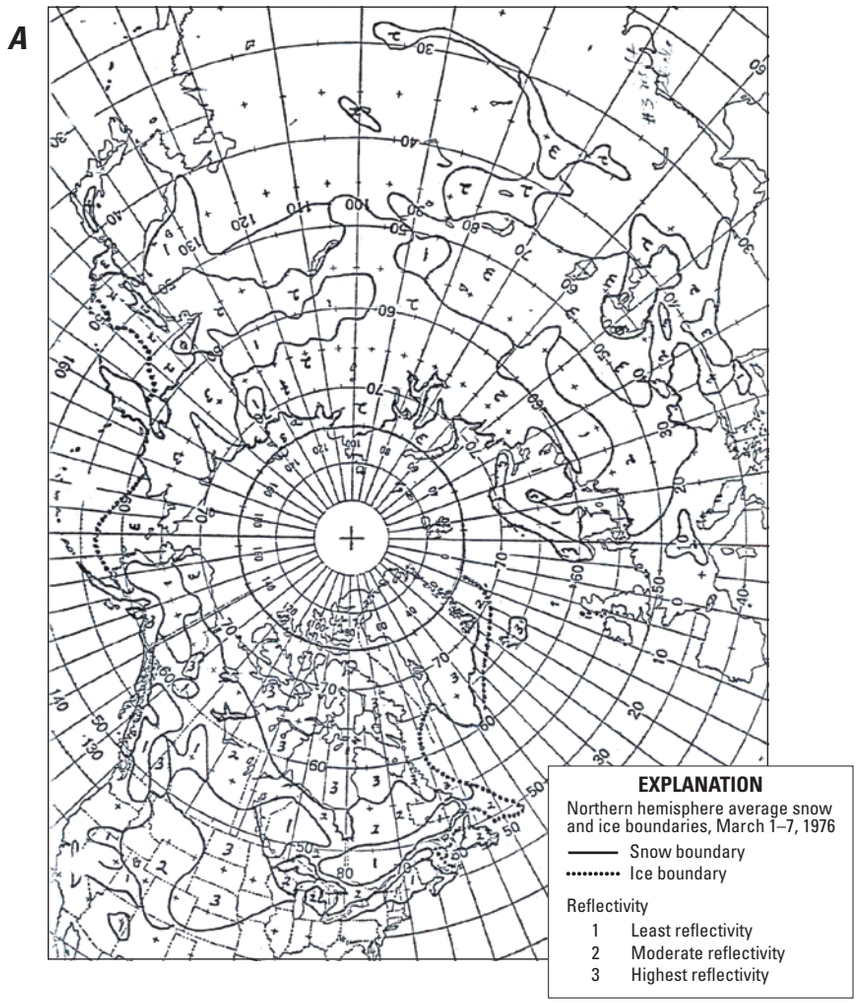

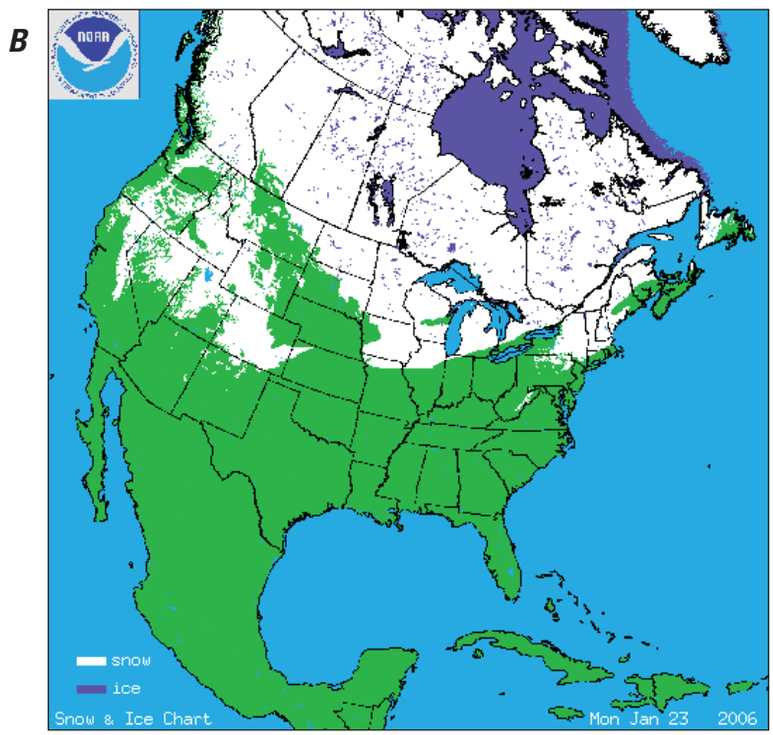

Figure 4.—**A**, *National Oceanic and Atmospheric Administration National Environmental Satellite, Data, and Information Service (NOAA NESDIS) snow map. 1–7 March 1976;* **B**, *NOAA NESDIS Interactive Multisensor Snow and Ice Mapping System (IMS) snow map, 23 January 2006. Snow cover is shown in white; sea and lake ice is shown in dark blue.*

Calculation of Snow-Cover Extent by Use of NOAA/NESDIS Maps

Weekly areas of snow-cover extent (SCE) are derived from the digitized snow files and, subsequently, monthly values are obtained by weighting the weeks according to the number of days of a map week falling in the given month (Robinson, 1993a). Prior to the calculations, the digital files are standardized to a common land mask. Only those grid cells that contain more than 50 percent land are included.

In 2001, a correction to NOAA grid cells was introduced. Significant errors in grid-cell areas for the lower-resolution NOAA grid had long been suspected. Documentation for the calculation of the cell-area file (which dates back to at least the late 1970s) has never been located. Therefore, cell areas in the 128×28 grid were recalculated by application of the general quadrilateral with spherical geometric relations in a polar stereographic projection (Smart and Green, 1977; Kidwell, 1998; Robinson and others, 2001). Overall, the revised, more accurate grid-cell areas are somewhat larger than the older areas. Revised cell areas are within about 1 percent of the former values, except equatorwards of 30°N. and polewards of 80°N., where they differ by as much as 3 percent. However, it is worth noting that snow rarely covers the ground in the southern region, and there is not much land north of lat 80°N. (principally northern Greenland and Ellesmere Island).

SCEs calculated from the new, revised cell areas ranges from 0.6 to 1.2 percent more than those listed in past reports. Percent differences are larger in the midspring through midfall. However, given that SCE is lower during this interval, adjusted extents are larger in the winter (as much as 0.30×10^6 km^2) than in summer (0.05×10^6 km^2).

MODIS-Derived Snow Maps

With the launch of NASA's Terra satellite, snow maps have been produced globally, from automated algorithms from the MODIS instrument since 24 February 2000 (Hall and others, 2002). The 4 May 2002 launch of the Aqua satellite put a second MODIS into operation, resulting in more snow-mapping opportunities each day. The MODIS snow products [*http://modis-snow-ice.gsfc.nasa.gov/*] come in a variety of spatial and temporal resolutions (figs. 5, 6) and projections to serve different user groups (Hall and Riggs, 2007). Daily, 8-day, and monthly composite snow maps with fractional snow cover are available at 500-m and 0.05° resolution. For modelers and others interested in a product at a coarser resolution, a 0.25°-resolution product also is available (Riggs and others, 2005).

The overall absolute accuracy of the well-studied 500-m resolution swath and daily tile products is approximately 93 percent under cloud-free conditions, but varies by land-cover type and snow condition (Hall and Riggs, 2007). By far the greatest limitation of the MODIS snow products is due to snow/cloud-discrimination problems because of the conservative nature of the MODIS cloud mask. For example, the daily tile snow products showed an overall accuracy of 94.2 percent compared with 15 SNOpack TELemetry (SNOTEL) sites in a study done by Klein and Barnett (2003) in which they compared MODIS snow maps and SNOTEL measurements in the Upper Rio Grande Basin for the 2000–2001 snow season. (SNOTEL is an automated system to collect snowpack and related data in the western United States.)

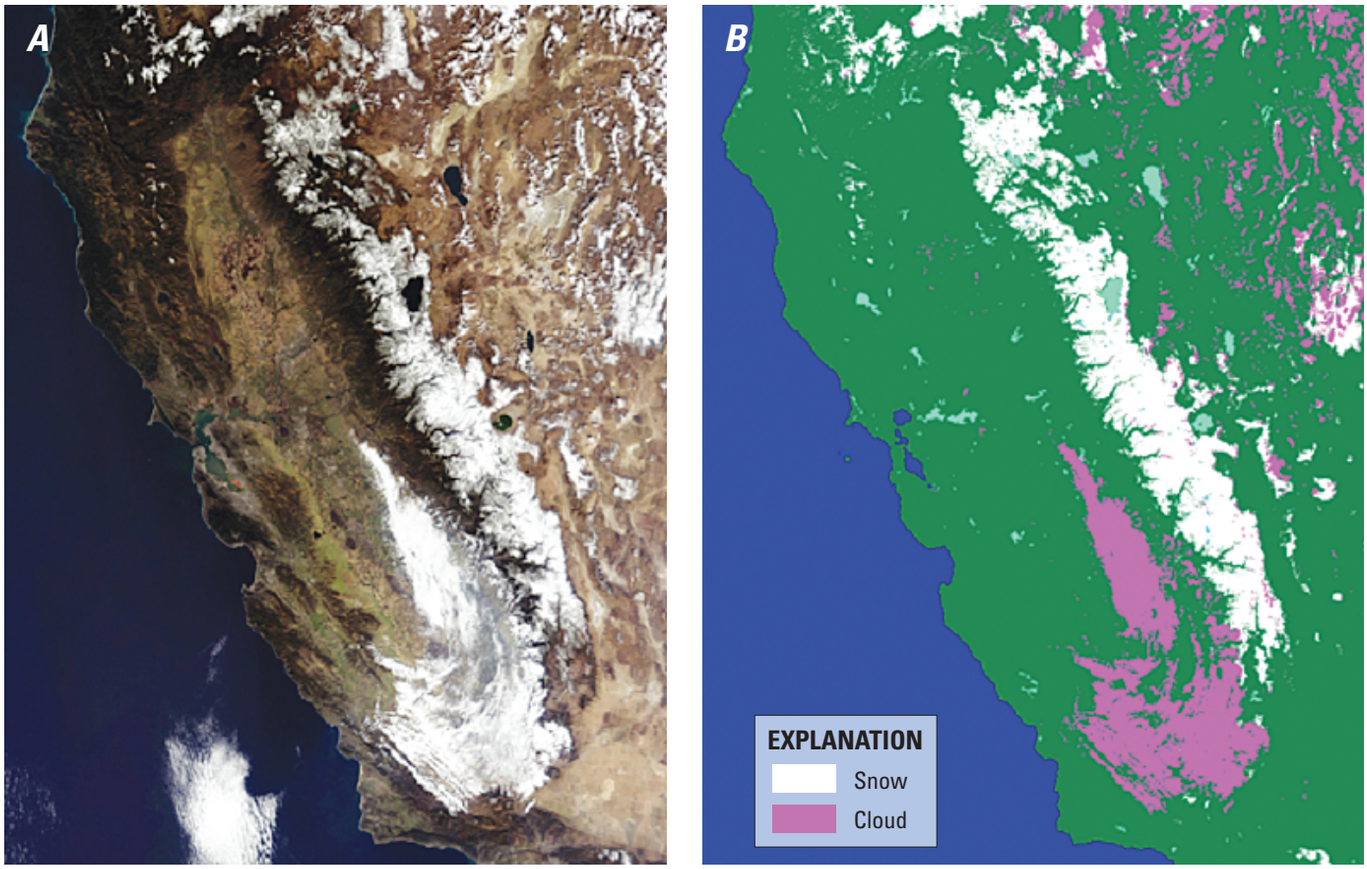

Figure 5.—**A**, *Moderate Resolution Imaging Spectroradiometer (MODIS) true-color image [bands 1 (620–670 nm), 4 (545–565 nm), and 3 (459–479 nm)]* and **B**, *MODIS snow map acquired on 31 October 2004. The area shown is in the western United States, including the Sierra Nevada in California.*

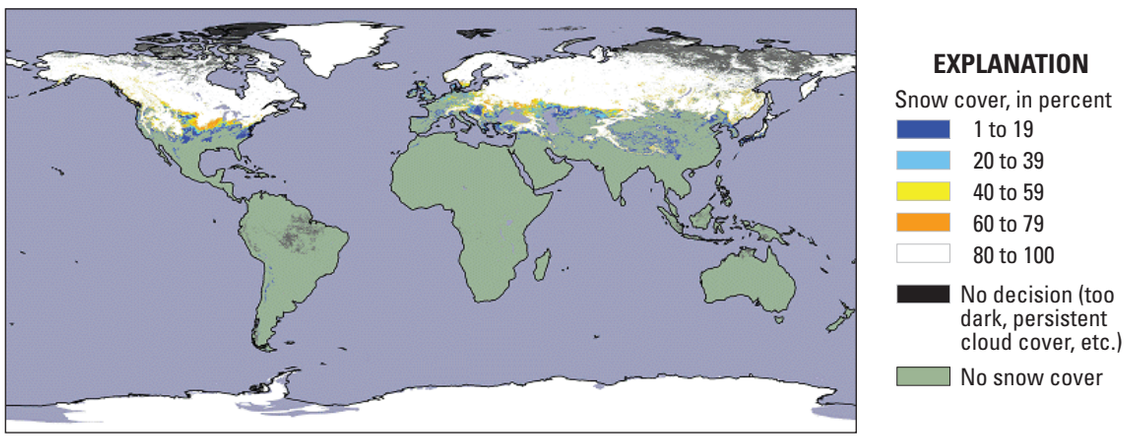

Figure 6.—*Moderate Resolution Imaging Spectroradiometer (MODIS) monthly snow map with fractional snow cover for February 2004. From MODIS Snow and Ice Project, NASA/Goddard Space Flight Center. [*http://modis-snow-ice.gsfc.nasa.gov*].*

Detection of very thin snow (< 1 cm) can also be problematic, especially over vegetated terrain. In addition, the accuracy of the MODIS snow products is lower in dense forest cover as discussed in Simic and others (2004).

NOAA/NOHRSC Snow Maps

The National Operational Hydrologic Remote Sensing Center (NOHRSC) snow-cover maps generated by National Weather Service (NWS) NOHRSC hydrologists are distributed electronically in near-real time to local, State, and Federal users during the North America snow season (Carroll, 1987, 1995; Carroll and others, 2001; [*http://www.nohrsc.nws.gov/nsa/*]). The NOHRSC 1-km maps are generated primarily from the NOAA POES and GOES satellites to develop daily digital maps depicting the areal extent of snow cover for the conterminous United States, Alaska, and parts of southern Canada. NOHRSC produces snow products and information that include estimates of SWE, snow depth, snowpack temperatures, sublimation, evaporation, and blowing snow; modeled and observed snow information; airborne snow data; satellite snow cover; historical snow data; and time series for selected modeled snow products.

Snow Mapping in the Microwave Part of the Electromagnetic Spectrum

In the microwave part of the spectrum (300- to 1-gigahertz (GHz) frequency, or 1-mm to 30-cm wavelength), snow cover from space is studied by measuring emitted radiation with a radiometer (passive) or by measuring the intensity (in decibels) of the return of a signal sent by a radar or by a scatterometer (active). Measurements can be made through darkness and can often be made through nonconvective clouds. Although the utility of microwave data for snow-cover studies has been demonstrated, significant limitations remain. For example, if the snow layer is very thin and dry, it may not scatter or reflect microwave radiation and thus may not be detected as snow. Moreover, a wet snowpack radiates like a blackbody at the physical temperature of the snow layer and is therefore indistinguishable from snow-free soil (Kunzi and others, 1982). Vegetation, especially forest cover, causes more complications.

Passive-Microwave Remote Sensing

Microwave emission from a layer of snow over a ground medium consists of two contributions: (1) emission by the snow volume and (2) emission by the underlying ground. Both contributions are governed by the transmission and reflection properties of the air-snow and snow-ground interfaces, by the absorption/emission and scattering properties of the snow layer (Stiles and others, 1981), and by a myriad of physical parameters that affects the emission (Derksen and others, 2002). The strength of the microwave emission is measured in brightness temperature, T_B, which is a measure of the intensity of radiation thermally emitted by an object. T_B is given in units of temperature because there is a correlation between the intensity of the radiation emitted and physical temperature of the radiating body. As an electromagnetic wave emitted from the underlying surface propagates through a snowpack, it is scattered by the randomly spaced snow particles in all directions. As the snowpack grows deeper, there is more loss of radiation due to scattering, and the emis-

sion of the snowpack is reduced, thus lowering the T_B. The deeper the snow, the more ice crystals or grains are available to scatter the upwelling microwave energy; because of this relationship between microwave energy and number of snow grains, it is sometimes possible to estimate the depth and SWE from microwave emission.

Volume scattering increases with snow-grain size and internal layering and with an increase in the amount of snow. Radiation at wavelengths comparable in size to the snow-crystal size (about 0.05 to 3.0 mm, or greater if depth hoar is present) is scattered in a dry snowpack and can be modeled according to Mie scattering theory (Chang and others, 1987). (Mie scattering predominates when the particles causing the scattering are larger than the wavelengths of radiation in contact with them.)

Active-Microwave Remote Sensing

Active-microwave remote sensing is useful for snow-cover mapping and for estimation of SWE. "Active" refers to the fact that a signal is sent from an instrument on an aircraft or satellite, and that signal interacts with the surface or near-surface and is then redirected back to the sensor, wherein the altered signal is recorded. Active-microwave remote sensing includes SAR and scatterometry.

A radar sends out a pulse of energy in the microwave part of the electromagnetic spectrum and records the energy that is reflected back. At the Earth's surface, the energy in the radar pulse is scattered in all directions, with some reflected back toward the antenna. This backscatter returns to the sensor as a weaker signal, because a radar image captures only the energy that is reflected back towards the radar antenna. SAR refers to a technique used to synthesize a very long antenna by combining backscatter received by the radar as the sensor moves along a flight track. X-band (frequency of 8.0–12.5 GHz, wavelength of 2.4–3.75 cm) or lower frequencies (longer wavelengths) are not generally useful for detecting and mapping thin, dry snow because the size of snow particles is much smaller than the size of the wavelength; at these longer wavelengths, there is little chance for a microwave signal to be attenuated and scattered by the relatively small ice crystals composing a snowpack (Waite and MacDonald, 1970; Ulaby and Stiles, 1981). The potential to measure SCE and SWE from space by means of spaceborne SARs exists, but only if higher frequency SARs, such as those at Ku-band (for example, 13.99-GHz frequency or 2.14-cm wavelength) are flown (Waite and MacDonald, 1970; Papa and others, 2002).

However, in the case of wet snow (Stiles and Ulaby, 1980; Ulaby and Stiles, 1981; Rott, 1984; Ulaby and others, 1986), when at least one layer of the snowpack (within the penetration depth of the radar signal) becomes wet (4–5 percent liquid water content), the penetration depth of the radar signal is reduced to about 3 to 4 cm (or one wavelength at X-band) (Mätzler and Schanda, 1984). Therefore, there may be high contrast between snow-free ground and ground covered with wet snow if somewhat lower frequency or longer wavelength SARs are used, making it possible to distinguish wet and dry land from wet snow (for example, when imaged with C-band SAR such as RADARSAT at 5.3-GHz frequency or 5.6-cm wavelength) for mapping SCE.

Scatterometry is useful for measuring snow depth and the extent of snowmelt because of its sensitivity to the presence of liquid water. A scatterometer is actually a microwave radar that is used specifically to measure the reflection

or scattering effect produced while scanning the surface of the Earth from an aircraft or a satellite. In the case of snow cover, backscatter from snow increases with increasing accumulation only up to a certain saturation depth, beyond which the microwaves cannot reach because of attenuation from dispersive loss in the snowpack (Nghiem and Tsai, 2001). Increasing snow depth leads to increasing backscatter. Satellite-borne scatterometry may be used to detect snowmelt and to measure the evolution of a snowpack, as shown by Nghiem and Tsai (2001) using the Ku-band NASA Scatterometer (NSCAT). Backscatter patterns reveal boundaries that correspond to the various snow classes delineated by Sturm and others (1995) (fig. 7). Additionally, they show rapid changes in the backscatter such as those that took place over the northern plains of the United States and the Canadian prairies that led to the major spring 1997 floods in the midwestern United States and southern Canada.

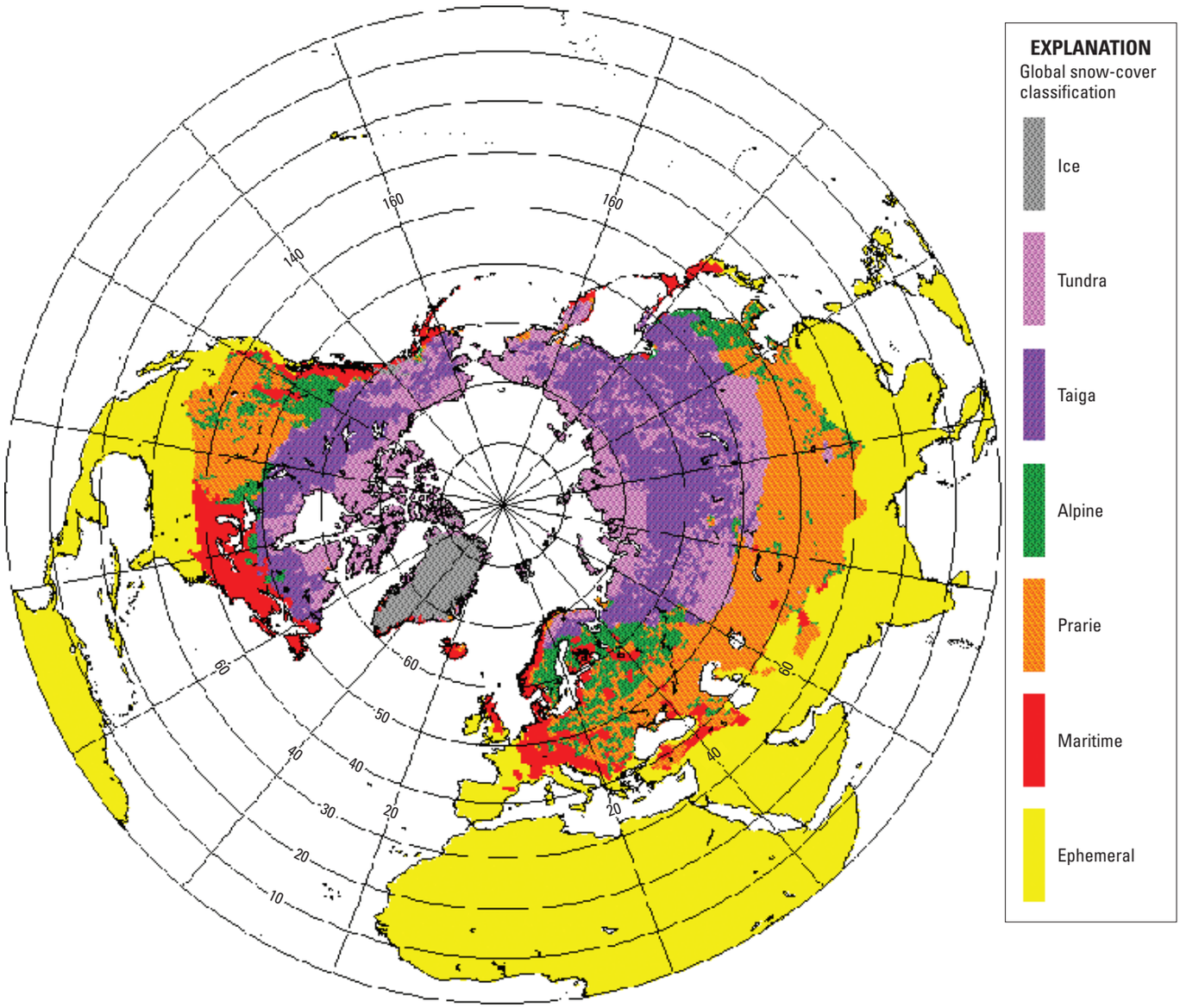

***Figure 7.**—Global snow-cover classification according to bioclimatological regions (Sturm and others, 1995). Image courtesy of National Snow and Ice Data Center, Boulder, Colo.*

Snow Maps Derived from the Microwave Part of the Spectrum

Snow maps showing both SCE and SWE (fig. 8) have been produced from passive-microwave sensors beginning in 1979 (Chang and others, 1987). Using passive-microwave data, first from the Scanning Multichannel Microwave Radiometer (SMMR) and more recently from the Special Sensor Microwave/Imager (SSM/I), Environment Canada has been producing SWE maps of the Canadian Prairies since the late 1970s (see [*http://www.socc.ca/examples/nsisw/ssmi/ccinprairies.jsp*]). These maps, an example of which is shown in figure 9, are used operationally to predict availability of water resources in the Canadian Prairies [*http://www.socc.ca/snow/snow_current_e.cfm*] (Walker and Goodison, 1993; Goodison and Walker, 1994) and in western Canada (Derksen and others, 2005).

Two significant advantages of using microwave sensors for snow mapping are that (1) data can be acquired during darkness or through cloud cover and (2) information about the snowpack, such as SWE, may be acquired. An important limitation of using passive-microwave data is the relatively low pixel resolution available from satellite data. In addition, the microwave data can be difficult to interpret because so many factors influence the T_B or backscatter.

The National Snow and Ice Data Center (NSIDC) produces a "Global Monthly EASE-Grid Snow Water Equivalent Climatology." This dataset contains global, monthly satellite-derived SWE climatologies gridded to the Northern and Southern 25-km Equal-Area Scalable Earth Grids (EASE-Grids). Global SWE is derived from SSM/I sensors (Armstrong and others,

***Figure 8.**—Passive-microwave-derived monthly mean snow map of South America for July 1991, based on the Chang and others (1987) Special Sensor Microwave/Imager (SSM/I) algorithm. Snow-water equivalent is shown on the maps in various shades of grey from 0 to 150 mm. Map courtesy of James L. Foster, NASA/Goddard Space Flight Center.*

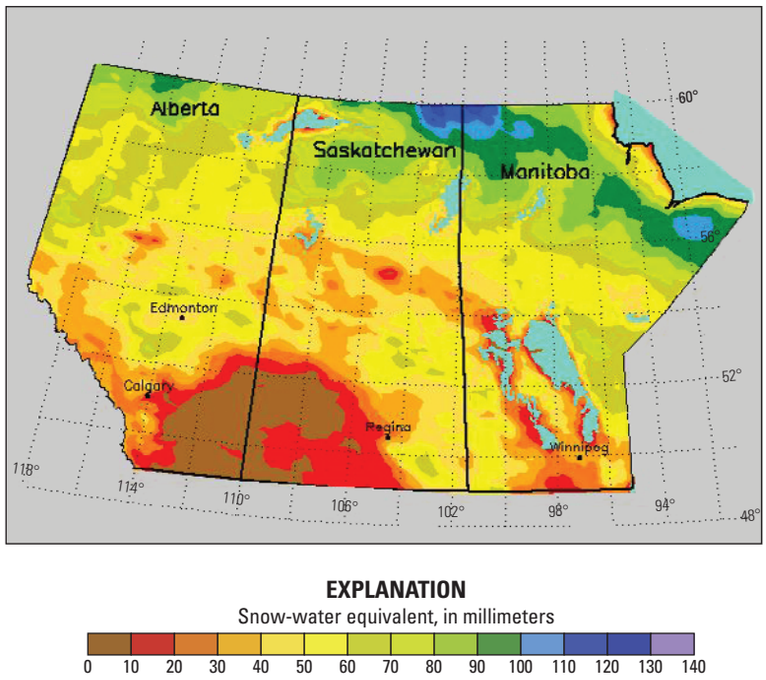

***Figure 9.**—Map of snow-water equivalent of the Canadian Prairies for 5 February 2002 derived from passive-microwave data. Map courtesy of Environment Canada.*

2005). These data are suitable for continental-scale time-series studies (1978 to present) of snow cover and SWE [*http://nsidc.org/data/nsidc-0271.html*]; however, in some terrain, the errors in SWE can be quite large. The Advanced Microwave Scanning Radiometer-Earth Observing System (AMSR-E) instrument on the NASA EOS Aqua satellite provides global passive-microwave measurements of SWE. Kelly and others (2003, 2004) developed a methodology using SSM/I and simple statistical-growth models to estimate snow grain size and density as a snowpack evolves through the season. These estimated variables are then coupled with a dense-media, radiative-transfer model to estimate SWE. The snow maps have been available as daily, pentad, and monthly SWE maps of the Northern and Southern Hemispheres at 25-km resolution on EASE-Grid since 19 June 2002. These data are available from NSIDC at [*http://nsidc.org/data/ae_dysno.html*].

Limitations of Snow Mapping from Space

There is no perfect sensor or combination of sensors for mapping SCE, depth, albedo, and SWE either from satellites or on the ground. Uncertainties exist in the remote sensing of snow cover, so validation with ground measurements is essential to improve the accuracy of satellite-derived measurements of SCE and SWE. Although satellite sensors see the big picture, point measurements or snow surveys along a transect on the ground fill in the needed details. However, owing to the high cost and difficulty of access of taking measurements in many remote and alpine locations, there are not enough ground measurements for full validation of satellite data. Interpolation between point measurements is necessary—and various statistical techniques can be used for this—but the validity of the interpolation is closely related to the density of ground measurements.

Acquisition of visible and near-infrared satellite observations is very often hindered by cloud cover and darkness, and dense vegetation may effectively block the view of the snow cover, leading to underestimation of snow-cover extent. One of the biggest issues in snow mapping in the reflective part of the spectrum is cloud screening (for example, see Riggs and Hall, 2003). Significant improvements in snow mapping will be gained by developing improved snow-cloud discrimination algorithms.

Emission and backscatter from dense vegetation influence satellite-based, passive-microwave measurements of snow cover because vegetation emits microwave radiation. The presence of vegetation, especially dense forests, causes passive-microwave SWE algorithms to underestimate snow depth because microwave emission from the trees raises the scene brightness temperature. Various techniques have been used to compensate for this problem (for example, see Hall and others, 1982; Hallikainen, 1984; Foster and others, 1997, 2005). Foster and others (2005) use percentage of forest cover (forest-cover fraction) to parameterize the effect of vegetation cover; the underestimation of SWE due to forest cover is parameterized empirically.

In short, satellite-borne sensors operating in the reflective part of the electromagnetic spectrum are very useful for SCE mapping but are limited by their inability to image through cloud cover and darkness, and dense vegetation may block the measurement of snow cover from space. Passive-microwave sensors are useful for measuring SCE, depth, and SWE; however, many factors limit the accuracy of these sensors for global snow mapping, and the spatial resolution of products derived from passive-microwave sensors is rather coarse.

Satellite-borne SARs are currently of little use for snow mapping because the C- and X-band wavelengths are too long relative to the size of the snow crystals to map dry snow effectively under a variety of conditions. However, the potential is great for snow and SWE mapping by use of SARs at shorter wavelengths or higher frequencies, such as Ku-band; and, in fact, Ku-band scatterometry has been shown to be useful for snow extent and depth mapping (Waite and MacDonald, 1970; Nghiem and Tsai, 2001).

Changes in the Northern Hemisphere Snow Cover During the Satellite Era

The mean annual Northern Hemisphere snow cover extent based on 1967–2005 records analyzed by the Rutgers GSL is 25.6×10^6 km^2. This includes snow over the continents, including over the Greenland ice sheet. The mean monthly area covered by snow ranges from a January maximum of 46.9×10^6 km^2 to 3.5×10^6 km^2 in August (table 1). Snow covers an average of more than 33 percent of land areas north of the Equator from November to April, reaching 49 percent coverage in January. In midwinter, approximately 60 percent of the hemispheric snow cover lies in Eurasia. Higher elevations on many glaciers and ice caps and on the Greenland ice sheet remain snow covered throughout the year.

From year to year, January snow cover may vary by 8×10^6 km^2. October snow cover has varied by 13×10^6 km^2 and April snow cover by more than 7×10^6 km^2. Less extensive July snow cover has varied by 5.5×10^6 km^2; however,

Table 1.—Monthly and annual climatological information on Northern Hemisphere snow extent between November 1966 and December 2005

[Data from Rutgers University Global Snow Lab. Years, number of years of data were used in the calculations. Extreme maximum and minimum values are followed by year of occurrence. The years 1968, 1969, and 1970 are missing 1, 6, and 5 months of data, respectively, and thus are not included in the annual calculations]

	Years	Area of snow extent, in millions of square kilometers					
		Mean	Standard deviation	Minimum	Year	Maximum	Year
January	39	46.9	1.5	42.1	1981	50.1	1985
February	39	45.9	1.9	42.9	1995 2002	51.4	1978
March	39	41.0	1.9	37.3	1990	44.5	1985
April	39	31.4	1.8	28.3	1968	35.7	1979
May	39	20.5	1.9	16.7	1968	24.4	1974
June	38	11.0	2.1	7.4	1990	15.8	1978
July	36	4.9	1.4	3.0	2005	8.7	1967
August	37	3.5	1.0	2.3	1968	5.8	1967 1968
September	37	5.7	1.0	4.0	1968 1990	8.0	1972
October	38	18.3	2.6	13.1	1988	26.3	1976
November	40	34.1	2.1	28.6	1979	38.7	1993
December	40	43.5	1.8	37.8	1980	46.3	1985
Annual	36	25.6	1.0	23.4	1990	27.6	1978

there remains some uncertainty as to whether the more extensive summer cover mapped in the 1970s is real or is the result of the analysts' inexperience. (Summer cloudiness in the high latitudes can make it difficult to distinguish clouds from snow-covered ground.) Training and imagery of higher quality led to more consistent mapping techniques in the 1980s and beyond. Monthly standard deviations range from 1.0×10^6 km^2 in August and September to 2.6×10^6 km^2 in October. Standard deviations are generally slightly below 2×10^6 km^2 during nonsummer months.

Maps depicting monthly climatologies may be viewed at the Rutgers GSL snow Web site [*http://climate.rutgers.edu/snowcover*]. This site also includes individual weekly and monthly maps, maps showing monthly anomalies (departures from long-term means) from November 1966 through June 2000, and daily products since mid-1999. Monthly areas for the Northern Hemisphere, Eurasia, and North America, the contiguous United States, Alaska, and Canada also are posted (fig. 10).

Regional warming has been measured in many areas of the Arctic (Serreze and others, 2000; Arctic Climate Impact Assessment, 2004, 2005). Temperature-albedo feedback, where the lower albedo resulting from snowmelt promotes additional surface warming (Groisman and others, 1994), is one reason why the Arctic is warming and is related, in part, to the observed decrease in Northern Hemisphere snow cover (Robinson and others, 1993; Brown and Braaten, 1998), to be discussed in a later section. Foster (1989) and Foster and others (1992) discussed a trend toward earlier snowmelt in Arctic

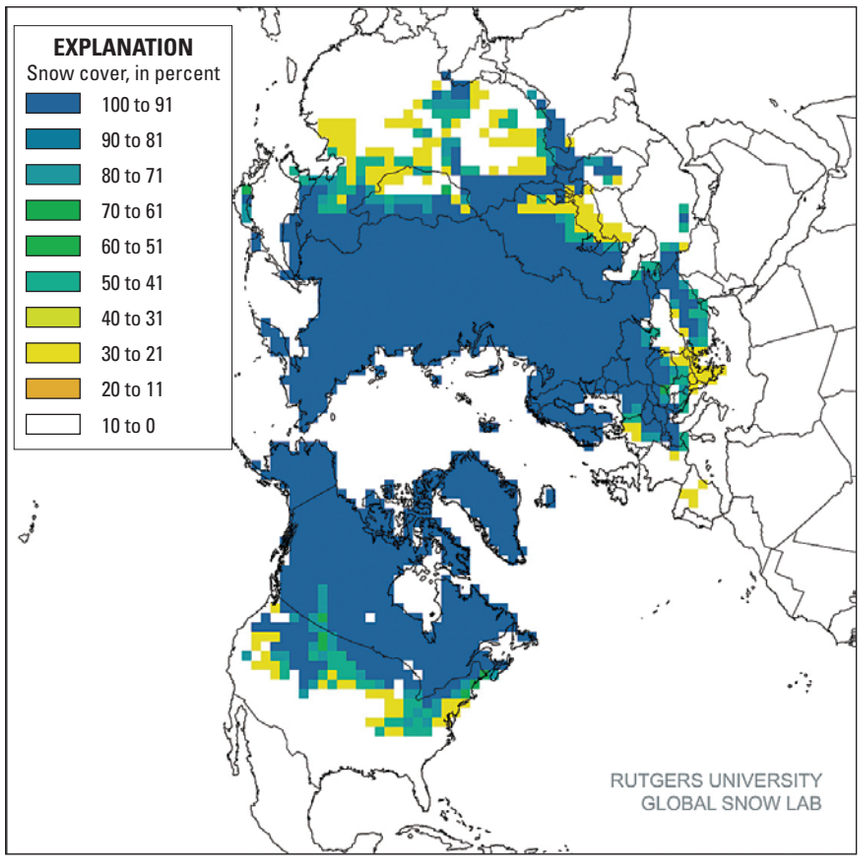

***Figure 10.**—Rutgers University Global Snow Lab monthly snow map for February 2006, based on NOAA/NESDIS snow maps, showing snow-cover frequency.*

locations; Stone and others (2002) extended that work, concluding that, on average, the spring snowmelt in northern Alaska is about 8 days earlier than in the mid-1960s.

Snow cover was more extensive during the first two decades of the satellite record than during the most recent two decades (fig. 11). As first reported in 1990 (Robinson and Dewey, 1990), snow cover since the late 1980s continues to be less extensive than it was during much of the earlier satellite era. Between 1967 and 1987, annual means of snow extent fluctuated around a mean of 26.1×10^6 km^2. A rather abrupt transition occurred between 1986 and 1988, and since then the mean annual extent has been 24.6×10^6 km^2. Means of these two periods are significantly different (t test, $p < 0.01$). Monthly anomalies from the long-term mean are most often less than 3×10^6 km^2, but on occasion they are as much as 4 or 5×10^6 km^2, with October 1976 having a positive anomaly of 8.3×10^6 km^2.

Recent SCE decreases in the Northern Hemisphere are large during the late winter to early summer, whereas fall and early-winter to midwinter SCE shows no statistically significant change. For example, April snow cover across both continents was more extensive in the 1967–87 period than from 1988 to the present. The tendency towards less late-season snow cover in recent years begins in February. During 8 of the first 20 years of record, February snow extent exceeded the January value. This has occurred only once since then.

Even in years when the annual SCE over Northern Hemisphere lands is close to average, SCE for many individual months is not close to average. Conditions in 2002 are a good example. The annual Northern Hemisphere SCE was 25.4×10^6 km^2, just 0.2×10^6 km^2 less than the long-term (1966–2005) mean. The area covered by snow in 2002 ranged from 46.9×10^6 km^2 in January 2002 to 2.7×10^6 km^2 in August 2002. Near-record low SCE was observed in February and March 2002, and a record low was reached in July 2002. The former two months ranked third and second lowest, respectively, based on 39 years of observations dating back to 1967. A completely different picture emerged late in 2002 with October, November, and December each ranking among the top five highest during the satellite era. The October positive anomaly of 5.2×10^6 km^2, 28 percent above average, is the second largest anomaly in terms of absolute snow area on record for any month since observations began in November 1966. The widely different picture from winter to fall is illustrated in figures 12 and 13, which show anomaly maps for February and October 2002.

Snow-cover extent (SCE) over both Eurasia and North America contributes to the lower post-1987 hemispheric extent (fig. 11). SCE for both was exceedingly low in the late 1980s and 1990s but rebounded somewhat by the mid-1990s. Since then, Eurasian SCE has fluctuated closer to the long-term mean than has North American SCE, which has averaged lower than the long-term mean.

During any particular month, SCE anomalies over Eurasia and North America may be in or out of synchronicity. For instance, in February 2005, Eurasian SCE was the third largest of record, whereas North America SCE ranked thirty third. Lower than average North American SCE was maintained throughout the spring, and it was not until May 2005 that Eurasian SCE decreased to well below average. December 2005 SCE was quite extensive over both continents, following a November when it ranked quite low for both.

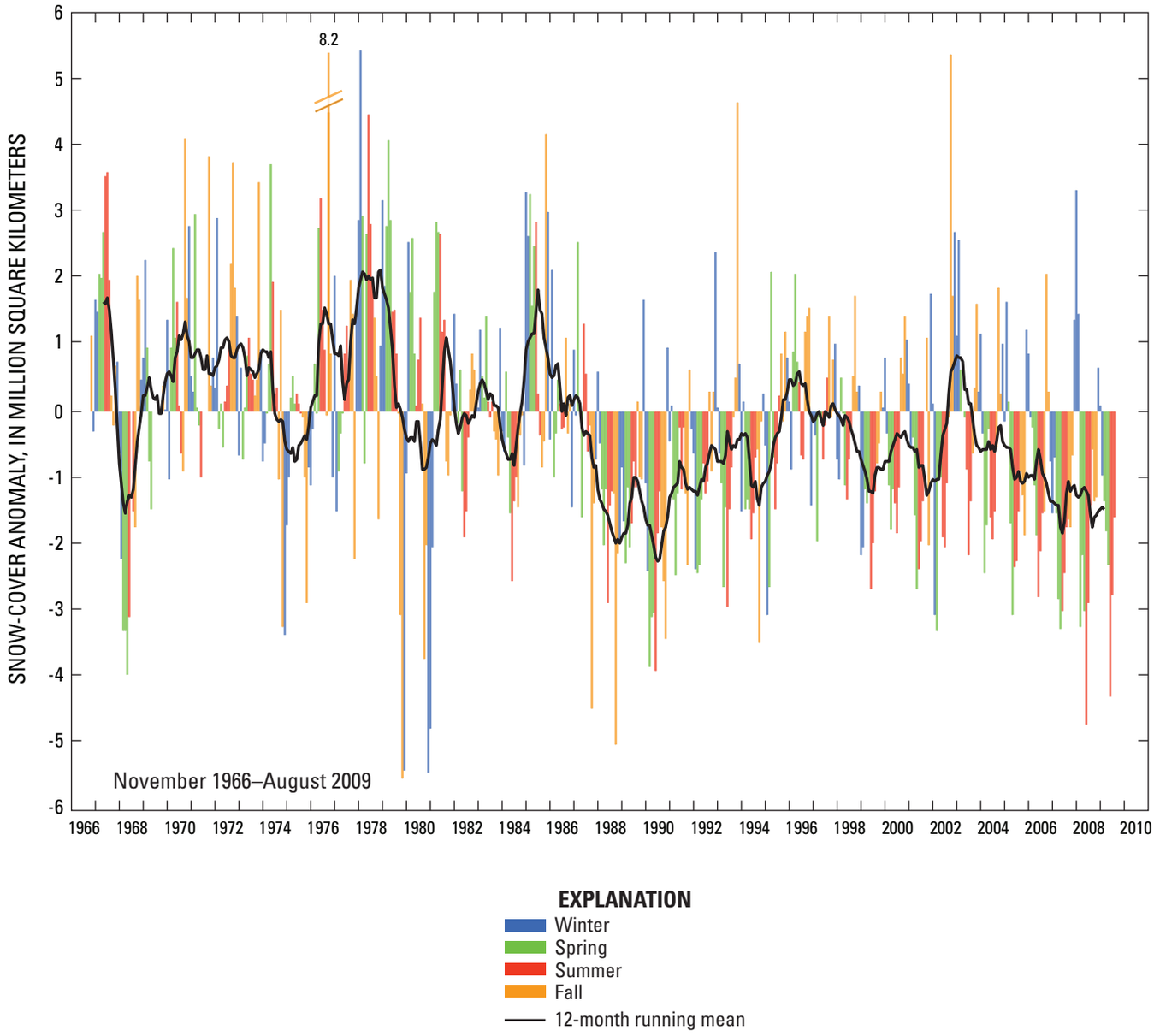

Figure 11.—*Rutgers University Global Snow Lab Northern Hemisphere snow-cover anomalies: November 1966–August 2009.*

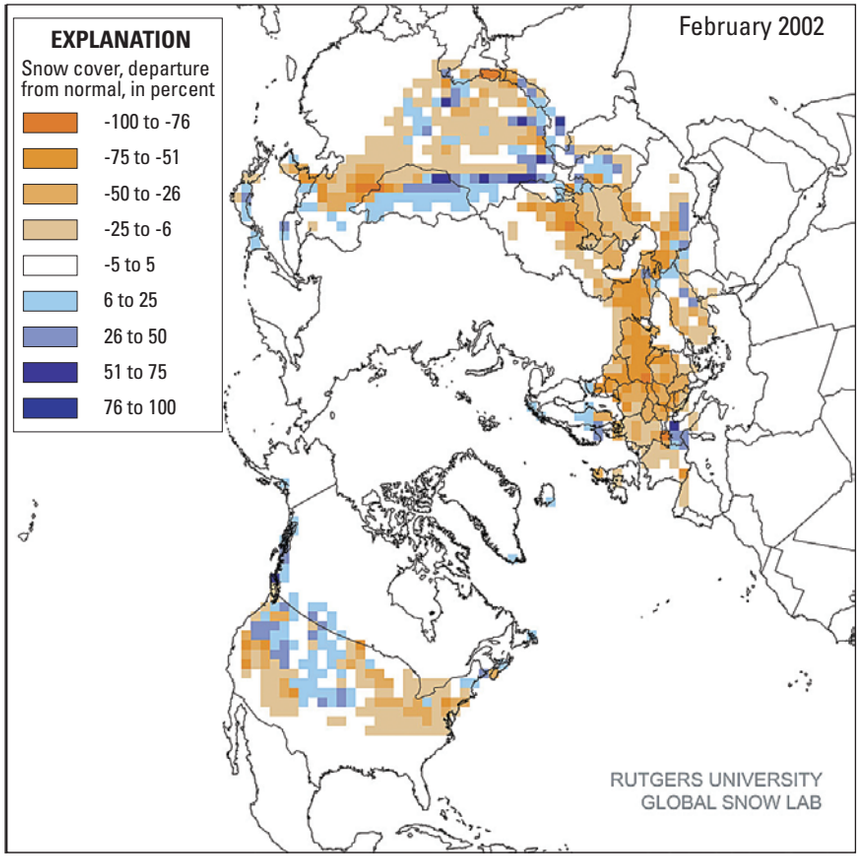

Figure 12.—*Rutgers University Global Snow Lab monthly snow map for February 2002, based on NOAA/NESDIS snow maps, showing snow-cover departure from normal.*

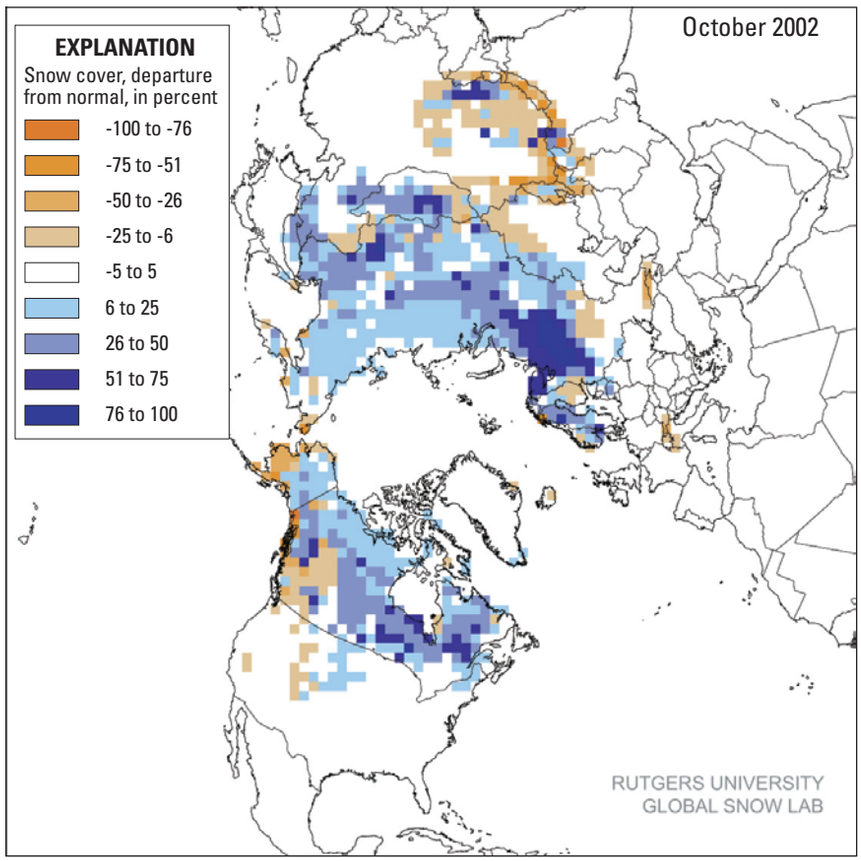

Figure 13.—*Rutgers University Global Snow Lab monthly snow map for October 2002, based on NOAA/NESDIS snow maps, showing snow-cover departure from normal.*

Variability in the Southern Hemisphere Snow Cover During the Satellite Era

Although snowfall occurs more frequently in the Northern Hemisphere than in the Southern Hemisphere, seasonal snow cover is an important factor in several regions of the Southern Hemisphere as well, particularly South America. Seasonal snow cover may be present on parts of the continents of Africa and Australia, and New Zealand has a large amount of seasonal snow cover (fig. 3). Snow cover can be present close to the Equator at high elevations, as is the case in South America, Africa, and Irian Jaya, Indonesia; all three regions have glaciers at the highest elevations. More than 98 percent of the continent of Antarctica is snow covered (snow cover on glacier ice); however, interannual variability is not as large as it is in South America. A brief discussion of satellite measurements of snow cover in the Southern Hemisphere follows.

Snow Cover in South America

An extensive, non-alpine seasonal snow cover forms in South America, south of lat 27°S. (Foster and others, 2001). In southern Argentina, snow may accumulate as early as May and as late as October. Snow cover is normal south of about 45°S. each winter (Patagonia and Pampas regions) in Chile and Argentina, and there can be a large variability in snow-covered area, both monthly and interannually.

Year-to-year variations in SCE over South America can be significant. From 1992 to 1998, the maximum amount of snow cover was recorded in 1992, and the year with the least amount of snow was 1996 according to an analysis by Foster and others (2001) using SSM/I data from May through August. July 1992 was the month with the greatest SCE (nearly 0.8×10^6 km^2) and snow mass (approximately 2.58×10^{13} kg).

Dewey and Heim (1983) reported that the maximum wintertime SCE in South America ranged from 692,000 km^2 to 1,011,000 km^2 between 1974 and 1980. More recent measurements based on GOES and MODIS satellite data indicate that those measurements may represent an overestimation of the maximum amount of snow cover in South America.

On the basis of MODIS data from 2000 to 2005, the maximum snow-covered area in South America during this period (table 2) was in 2002 (619,515 km^2, when snow-cover fractions of 10 to 100 percent were mapped). Measurements were made from maps of monthly maximum snow cover from July in each year at approximately 25-km pixel resolution (though pixel data at higher resolution pixel also are available from MODIS and could be used for a still more accurate measurement). This SCE is lower than the range reported by Dewey and Heim (1983) but, of course, different years were studied. Romanov and Tarpley (2003) mapped snow cover in South America from the GOES satellite at approximately 4-km pixel resolution. Their measurements also showed less wintertime snow cover in South America than was found by Dewey and Heim (1983) although, again, different years were studied. For the years 2000 and 2001, Romanov and Tarpley (2003) reported that the wintertime snow cover reached about 620,000 km^2 and 670,000 km^2, respectively. The possible discrepancies in maximum snow cover measured by Dewey and

Table 2.—Approximate maximum percentage of snow-covered area in South America in July

[As measured using 0.25° resolution MODIS Climate-Modeling Grid snow-cover maps composited for the entire month for all grid cells and those that were 10 percent and 20 percent or greater covered by snow]

Year	Percentage		
	1–100	10–100	20–100
2000	536,011	492,691	442,449
2001	435,255	393,119	350,011
2002	656,096	619,515	571,323
2003	420,899	385,933	339,128
2004	403,828	363,119	311,983
2005	485,724	459,168	424,479

Heim (1983) and more recent measurements using GOES and MODIS data might be explained by the inaccuracy of the early NOAA snow charts because of their coarse spatial resolution (approximately 180-km pixels) compared to the higher resolution pixel data available since then (Romanov and Tarpley, 2003, and MODIS data listed in table 2); alternatively, without additional information, we cannot ignore the possibility that the maximum SCE might have been greater between 1974 and 1980.

The MODIS (table 2) and GOES measurements do not agree in terms of the areal extent (square kilometers) or the pattern of snow cover for the years 2000 and 2001. MODIS measurements show less maximum snow cover in 2001 than in 2000, whereas the GOES measurements from Romanov and Tarpley (2003) show greater maximum snow cover in 2001 than in 2000. This may not mean that either is incorrect, however, because different time periods and methods were used to calculate the SCE in each case.

There has been a general increase in elevation of the snowline in most areas of South America since the end of the Little Ice Age in the late 1800s (Williams and Ferrigno, 1998). For example, snowfields and glaciers in Colombia are now restricted to the highest peaks and ranges of the Cordillera Central, Cordillera Oriental, and Sierra Nevada de Santa Marta (Hoyos-Patiño, 1998). Annual precipitation of snow in the highest cordillera is 1,200 to 2,500 mm of water equivalent, resulting in an annual accumulation of 2 to 3 m of snow between 5,000 to 6,000 m of elevation (Morales Arnao and Hastenrath, 1998). The eastern slopes of the Andes receive the greatest precipitation because of moisture from the vast Amazon Basin and the Atlantic Ocean.

Snow Cover in Australia, New Zealand, and Africa

In Australia, heavy mountain snowfalls may occur any time of the year, and snowfall in southeastern Australia may occur during wintertime. In the Australian Alps (lat 35–38°S.), winter snow cover generally lasts from a few weeks at elevations of 1,200 to 1,400 m up to 4 months or more at higher peaks

(1,800–2,000 m) (Whetton and others, 1996), but the snow-cover period is variable from year to year. The alpine area includes mountains in the States of Victoria and New South Wales.

In New Zealand, snowfall is most frequent during July and August but may occur at anytime of the year above 5,000 m (Dewey and Heim, 1983; Foster and others, 2001). The North Island of New Zealand has a small permanent snowfield above 2,500 m on the central plateau, but the snowline rarely descends below 600 m. Seasonal snow covers about 60,000 km^2 of New Zealand—more than 35 percent of South Island and some mountain areas of North Island (Fitzharris and McAlevey, 1999). Thus, the greatest extent of the seasonal snow cover is on South Island (fig. 3).

South Island is divided along its length by the Southern Alps, the highest peak of which is Aoraki/Mount Cook at 3,754 m. (There are 18 peaks of more than 3,000 m on the South Island.) On South Island, snowmelt constitutes as much as 50 percent of the water inflow to hydroelectric storage lakes (whereas meltwater from glaciers constitutes only 10 percent) (Fitzharris, 2004). On South Island, snow falls on a few days a year in the eastern coastal districts. In inland Canterbury and Otago, where there are considerable areas of grazing lands above 300 m, snowfalls are heavier and more persistent and have caused serious sheep losses during severe winters. In that area, however, it is rare for the winter snowline to remain below 1,000 m for extended periods (Meteorological Service of New Zealand [n.d.]). The snowline in the Southern Alps is about 2,000 m in summer, being slightly lower on the western side where the Franz Josef and Fox Glaciers descend through heavy bush to within 300 m of sea level (Chinn, 1989). Though there is a great deal of interannual variability in seasonal snow cover in New Zealand, there are no long-term snow-cover records (Fitzharris and Garr, 1995). Model results show that the timing of maximum snow storage in New Zealand varies significantly from year to year, with the maximum occurring later in larger snow years (late October or even in November); the minimum can occur as early as July (Fitzharris, 2004). Model results for the Southern Alps show that, on average, seasonal snow builds from about May to a maximum of 366 mm in October, but no long-term trend is apparent (Fitzharris and Garr, 1995).

In Africa, snow can fall close to the Equator at high elevations, such as on Mount Kilimanjaro (fig. 14), Mount Kenya, and the Ruwenzoris in Africa, all three of which host glaciers, and occasionally in northern Africa, such as occurred on 26 and 27 January 2005, in Algeria and Morocco. On Mount Kilimanjaro, the permanent ice cover decreased 80 percent from 1812 to 2000 (Thompson and others, 2002). Since the end of the Pleistocene Epoch, there has been a dramatic decrease in the glaciers of the mountains of Africa (Young and Hastenrath, 1991), owing to a decrease in precipitation in the late 19th century and a slight warming in the first half of the 20th century.

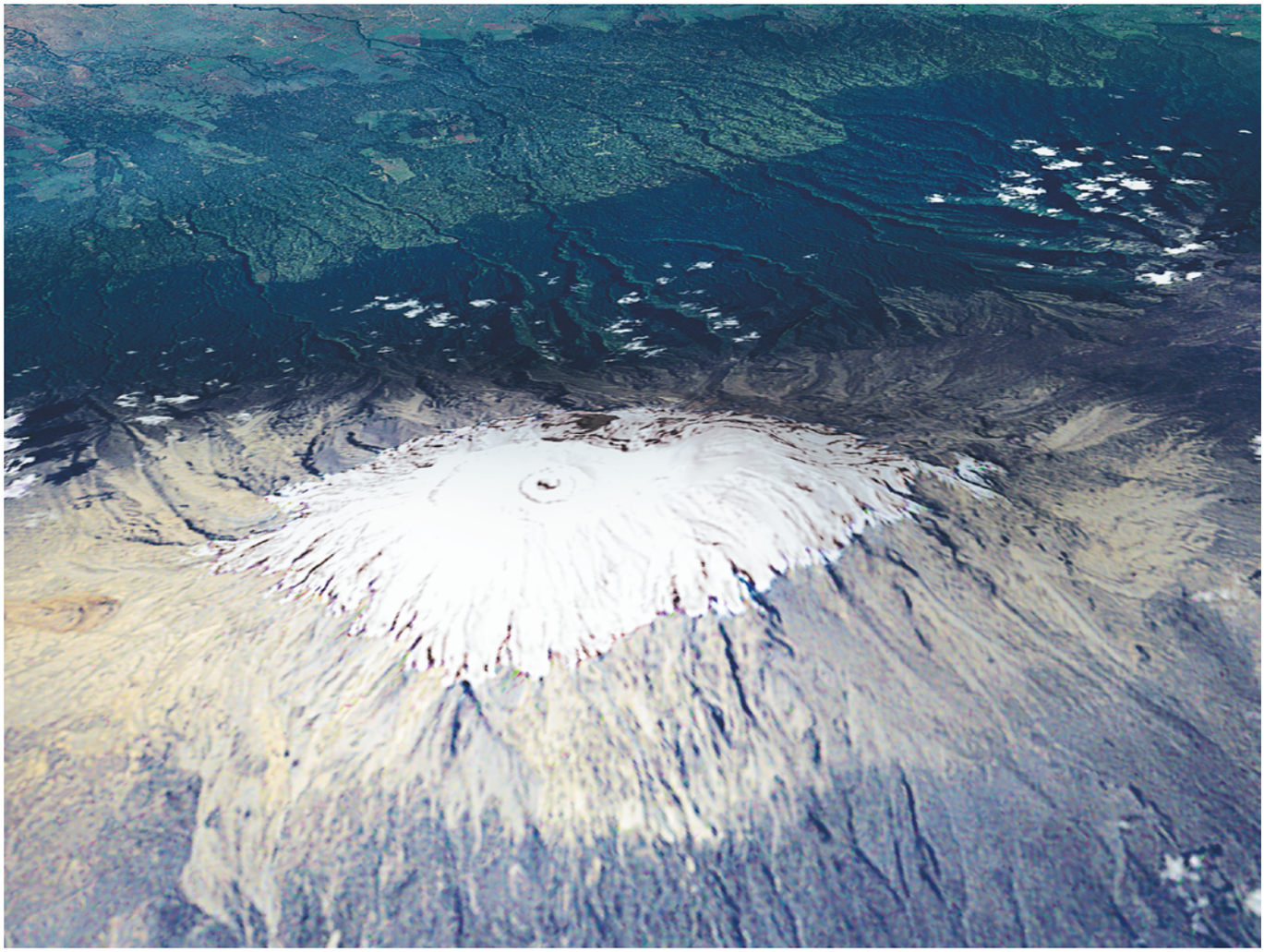

Figure 14.—*Glacier ice and snow on Mount Kilimanjaro, Tanzania, Africa, a 5,895-m high volcano. The image was acquired on 17 February 1993, by the Thematic Mapper on the Landsat-5 satellite and was draped over a digital elevation model to give an enhanced sense of the three-dimensional shape of the mountain. Image courtesy of NASA's MODIS Land Rapid Response Team.*

Development of Long-Term Data Records

Progress has been made toward the development of a satellite-era SCE climate-data record (CDR) for Northern Hemisphere lands that is based on NOAA/NESDIS visible maps. For many years, the Rutgers GSL version of this visible product has been used for studying snow-cover trends (National Academy of Sciences, 2004). At times, reanalysis of parts of the record have taken place (see discussion earlier in this chapter); recently, however, a more consistent record has been generated, taking into account notable changes in mapping that began in the late 1990s. Comparisons of the lower-pixel-resolution older NOAA product and the newer IMS product that were mapped independently between 1997 and 1999 were employed to generate adjustment factors. These adjustments were applied back in time (pre-June 1999, the standard being IMS) and forward in time (post-May 1999, the standard being the older NOAA product). This approach resulted in a large enough area coverage to be useful in accessing error margins. A standard land mask eliminated differences observed when the mapping change took place in 1999. This permitted fine tuning of the record. The broad continental and hemispheric assessments of snow extent that were done previously are still valid.

The MODIS snow-cover record (24 February 2000 to the present) is produced by means of algorithms that run in an automated-processing environment. The dataset has been reprocessed several times as algorithm improvements have been instituted. Currently, what is called Collection 5, or Version 5 is the most recent. Automated algorithms have limitations, but in terms of developing a CDR, they also have major advantages because even if an error is found in the algorithm that produces the dataset, the entire dataset can be reprocessed consistently. The consistency of the dataset is a critical feature of a CDR.

The development of a snow-cover CDR poses many challenges (see, for example, Hall and others, 2004). Many of those challenges have already been uncovered and discussed in terms of the NOAA/NESDIS snow-cover record. For example, the maps are produced manually and thus subject to different interpretation of SCE; different satellites were used to produce the maps during the period of record, and a variety of spatial resolutions was employed. In addition, the seamless stitching together of entirely different datasets—for example, the Rutgers and the MODIS SCE datasets—poses further challenges. There may never be long-term datasets that fit together seamlessly. Therefore, a key element of a CDR is that the errors will change over time (and hopefully be reduced) and that sources and magnitude of errors must be specified for each part of the CDR.

Conclusions

Much effort has gone into the measurement of snow cover from the ground and from space because of the influence of snow cover on the Earth's global climate and the key role of snow in providing water for human use. Progress has been made in quantifying the amount of water in a snowpack and in measuring interannual variability and trends in snow cover—especially in the Northern Hemisphere, where most of the seasonal snow cover is found. Visible, near-infrared, and microwave sensors are all useful for snow-cover measurements.

Interannual to multidecadal variability in Northern Hemisphere continental SCE has been monitored throughout the past 40 years of the satellite era. NOAA/NESDIS visible/near-infrared derived snow maps have been used since late 1966, and passive-microwave snow mapping began in 1979. Along with considerable interannual variations, a significant reduction in SCE extent occurred between the first two decades of observation and the most recent two. This reduction has been recognized over both Eurasia and North America and is evident from late winter to early summer.

Various studies based on satellite data, employing both visible/near-infrared and passive-microwave snow maps, show that the Northern Hemisphere annual snow-covered area has decreased (Robinson, 1993b; Brown and Goodison, 1996; Hughes and Robinson, 1996; Hughes and others 1996; Frei and others, 1999; Brown, 2000). Using passive-microwave snow maps, Armstrong and Brodzik (2001) showed a reduction of about 2 percent per year from 1978 to 1999. Since the late 1980s, SCE has declined in spring and summer but not substantially in winter. Whereas maximum SCE occurred frequently in February early in the satellite era, the seasonal maximum has occurred almost exclusively in January since the rather abrupt spring shift between 1986 and 1988. Between 1967 and 1986, mean annual SCE was 24.4×10^6 km^2. Since 1988, the mean annual extent has been 23.1×10^6 km^2, a statistically significant (t test, $p < 0.01$) reduction of approximately 5 percent (Robinson and Frei, 2000).

In the Southern Hemisphere, seasonal snow cover is greatest in South America, but it also occurs in Australia, New Zealand, and a few other mostly high-elevation locations (for example, in Africa and in Irian Jaya, Indonesia). The absence of sustained observations in the Southern Hemisphere makes it difficult to ascertain anything but the most general of knowledge regarding interannual variability of extent.

Enhancements to the current suite of sensors that measure snow cover will take place in the future, most likely in the active-microwave realm. Scatterometer data and Ku-band SAR data both have potential to refine measurements of snow-covered area even beneath cloud cover and to provide higher resolution snow-cover mapping in mountainous areas. With these sensors, great potential exists to improve the measurement of SWE. Similarly, increasing temporal and spatial resolution characteristic of visible and near-infrared sensors will result in increased detail in snow-cover maps. Visible, near-infrared, and microwave satellite data and ground measurements capable of ingest into hydrologic models will improve the derivation of SCE and SWE over time.

Because several decades of visible/near infrared and passive-microwave data of global SCE are now available, development of CDRs is now feasible. With the advent of MODIS global snow-cover maps in 2000 and future availability of maps from the National Polar Orbiting Environment Satellite System (NPOESS), the CDRs can be continued into the future. With these better controlled records, we should be able to detect trends, if applicable, in global snow cover and perhaps relate those trends to changing climate, thus improving our understanding of the complex relationship between global snow cover and global climate and climate change.

Acknowledgments

The authors thank Kimberly Casey, RSIS, and Nick DiGirolamo, Science Systems and Applications, Inc., for image creation and processing. We thank Jim Foster NASA/Goddard Space Flight Center, Richard Armstrong of the NSIDC, Ross Brown of the Meteorological Service of Canada, and Allan Frei of City College of New York/Hunter College for their technical reviews, which resulted in numerous improvements to the manuscript. George Riggs, Science Systems and Applications, Inc., provided much substantive information regarding the MODIS snow-cover products. Thanks also are extended to Don Garrett at the NOAA Climate Prediction Center for furnishing continuous updates of the raw digitized NOAA snow map data and to Tom Estilow for compiling and maintaining the snow database and Global Snow Lab Web site. Dorothy Hall's work is supported by NASA's Earth Observing System (EOS) Project and the Cryospheric Sciences Program at NASA. Dave Robinson's work is supported by three NOAA/NASA grants.

References Cited

Arctic Climate Impact Assessment, 2004, Impacts of a warming climate—Arctic Climate Impact Assessments: Cambridge, U.K., Cambridge University Press, 139 p. [*http://www.acia.uaf.edu*]

Arctic Climate Impact Assessment, 2005, Arctic climate impact assessment: Cambridge, U.K., Cambridge University Press, 1,042 p.

Armstrong, R.L., and Brodzik, M.J., 2001, Recent northern hemisphere snow extent—A comparison of data derived from visible and microwave satellite sensors: Geophysical Research Letters, v. 28, no. 19, p. 3673–3676.

Armstrong, R.L., Brodzik, M.J., Knowles, K., and Savoie, M., 2005, Global monthly EASE-Grid snow water equivalent climatology: Boulder, Colo., National Snow and Ice Data Center, digital data.

Barnett, T.P., Dümenil, L., Schlese, U., Roeckner, E., and Latif, M., 1989, The effect of Eurasian snow cover on regional and global climate variations: Journal of the Atmospheric Sciences, v. 46, no. 5, p. 661–686.

Bauer, K.G., and Dutton, J.A., 1962, Albedo variations measured from an airplane over several types of surface: Journal of Geophysical Research, v. 67, no. 6, p. 2367–2376.

Brown, R.D., 2000, Northern Hemisphere snow cover variability and change, 1915–97: Journal of Climate, v. 13, no. 13, p. 2339–2355.

Brown, R.D., and Braaten, R.O., 1998, Spatial and temporal variability of Canadian monthly snow depths, 1946–1995: Atmosphere-Ocean, v. 36, no. 1, p. 37–45.

Brown, R.D., and Goodison, B.E., 1996, Interannual variability in reconstructed Canadian snow cover, 1915–1992: Journal of Climate, v. 9, no. 6, p. 1299–1318.

Carroll, T.R., 1987, Operational airborne measurements of snow water equivalent and soil moisture using terrestrial gamma radiation in the United States, *in* Goodison, B.E., Barry, R.G., and Dozier, J., eds., Large scale effects of seasonal snow cover: International Association of Hydrological Sciences Publication 166, p. 213–223.

Carroll, T.R., 1995, Remote sensing of snow in the cold regions, in Proceedings, First Moderate Resolution Imaging Spectroradiometer (MODIS) Snow and Ice Workshop, Greenbelt, Md., 13–14 September 1995: National Aeronautics and Space Administration Conference Publication 3318, p. 3–14.

Carroll, Tom; Cline, Don; Fall, Greg; Nilsson, Anders; Li, Long; and Rost, Andy, 2001, NOHRSC operations and the simulation of snow cover properties for the conterminous U.S., in Proceedings, 69th Western Snow Conference, Sun Valley, Id., 16–19 April 2001, p. 1–10.

Chang, A.T.C., Foster, J.L., and Hall, D.K., 1987, Nimbus-7 SMMR derived global snow cover parameters: Annals of Glaciology, v. 9, p. 39–44.

Chinn, T.J.H., 1989, Glaciers of New Zealand, *in* Williams, R.S., Jr., and Ferrigno, J.G., eds., Satellite image atlas of glaciers of the world: U.S. Geological Survey Professional Paper 1386–H (Glaciers of Irian Jaya, Indonesia, and New Zealand), p. H25–H48. [*http://pubs.usgs.gov/pp/p1386h*]

Cohen J., and Entekhabi, D., 1999, Eurasian snow cover variability and Northern Hemisphere climate predictability: Geophysical Research Letters, v. 26, no. 3, p. 345–348.

Derksen, C., Walker, A., LeDrew, E., and Goodison, B., 2002, Time-series analysis of passive-microwave-derived central North American snow water equivalent imagery: Annals of Glaciology, v. 34, p. 1–7.

Derksen, C., Walker, A., and Goodison, B., 2005, Evaluation of passive microwave snow water equivalent retrievals across the boreal forest/tundra transition of western Canada: Remote Sensing of Environment, v. 96, nos. 3–4, p. 315–327.

Dewey, K.F., and Heim, R., Jr., 1983, Satellite observations of variations in Southern Hemisphere snow cover: National Oceanic and Atmospheric Administration, National Environmental Satellite, Data, and Information Service, Technical Report 1, 20 p.

Dirmhirn, Inge, and Eaton, F.D., 1975, Some characteristics of the albedo of snow: Journal of Applied Meteorology, v. 14, no. 3, p. 375–379.

Dozier, Jeff, 1989, Spectral signature of alpine snow cover from the Landsat thematic mapper: Remote Sensing of Environment, v. 28, no. 1, p. 9–22.

Dozier, Jeff, Schneider, S.R., and McGinnis, D.F., Jr., 1981, Effect of grain size and snowpack water equivalence on visible and near-infrared satellite observations of snow: Water Resources Research, v. 17, no. 4, p. 1213–1221.

Duguay, C.R., and LeDrew, E.F., 1992, Estimating surface reflectance and albedo from Landsat-5 thematic mapper over rugged terrain: Photogrammetric Engineering and Remote Sensing, v. 58, no. 5, p. 551–558.

Ferrigno, J.G., and Williams, R.S., Jr., 1983, Limitations in the use of Landsat images for mapping and other purposes in snow- and ice-covered regions—Antarctica, Iceland, and Cape Cod, Massachusetts, *in* Proceedings, 17th International Symposium on Remote Sensing of Environment: Ann Arbor, Mich., Environmental Research Institute of Michigan, v. 1, p. 335–355.

Fitzharris, B.B., and Garr, C.E., 1995, Simulation of past variability in seasonal snow in the Southern Alps, New Zealand: Annals of Glaciology, v. 21, p. 377–382.

Fitzharris, B.B., and McAlevey, B.P., 1999, Remote sensing of seasonal snow cover in the mountains of New Zealand using satellite imagery: Geocarto International, v. 14, no. 3, p. 33–42.

Fitzharris, B., 2004, Snow accounts for New Zealand: National Institute of Water and Atmospheric Research, Ministry for the Environment, and Statistics, New Zealand, 12 p. [*http://www.stats.govt.nz/NR/rdonlyres/12C962E5-B934-4BE3-A2BC-53EBD7ED3B50/0/snow.pdf*]

Foster, J.L., 1989, The significance of the date of snow disappearance on the Arctic tundra as a possible indicator of climate change: Arctic and Alpine Research, v. 21, no. 1, p. 60–70.

Foster, J.L., Owe, M., and Rango, A., 1983, Snow cover and temperature relationships in North America and Eurasia: Journal of Climate and Applied Meteorology, v. 22, no. 3, p. 460–469.

Foster, J.L., Winchester, J.W., and Dutton, E.G., 1992, The date of snow disappearance on the Arctic tundra as determined from satellite, meteorological station and radiometric in situ observations: Institute of Electrical and Electronic Engineers, Transactions on Geoscience and Remote Sensing, v. 30, no. 4, p. 793–798.

Foster, J.L., Chang, A.T.C., and Hall, D.K., 1997, Comparison of snow mass estimates from a prototype passive microwave snow algorithm, a revised algorithm and snow depth climatology: Remote Sensing of Environment, v. 62, no. 2, p. 132–142.

Foster, J.L., Chang, A.T.C., Hall, D.K., and Kelly, R., 2001, Seasonal snow extent and snow mass in South America using SSM/I passive microwave data: Polar Geography, v. 25, no. 1, p. 41–53.

Foster, J.L.; Sun, Chaojiao; Walker, J.P.; Kelly, Richard; Chang, Alfred; Dong, Jiarui; and Powell, Hugh, 2005, Quantifying the uncertainty in passive microwave snow water equivalent observations: Remote Sensing of Environment, v. 94, no. 2, p. 187–203.

Frei, Allan, and Robinson, D.A., 1999, Northern hemisphere snow extent—Regional variability 1972–1994: International Journal of Climatology, v. 19, no.14, p. 1535–1560.

Frei, Allan, Robinson, D.A., and Hughes, M.G., 1999, North American snow extent, 1900–1994: International Journal of Climatology, v. 19, no. 14, p. 1517–1534.

Goodison, B.E., and Walker, A.E., 1994, Canadian development and use of snow cover information from passive microwave satellite data, *in* Choudhury, B.J., Kerr, Y.H., Njoku, E.G., and Pampaloni, P., eds., Proceedings of the European Space Agency/National Aeronautics and Space Administration International Workshop, p. 245–262.

Greuell, Wouter; Reijmer, C.H.; and Oerlemans, Johannes, 2002, Narrowband-to-broadband albedo conversion for glacier ice and snow based on aircraft and near-surface measurements: Remote Sensing of Environment, v. 82, no. 1, p. 48–63.

Groisman, P. Ya., Karl, T.R., and Knight, R.W., 1994, Observed impact of snow cover on the heat balance and the rise of continental spring temperatures: Science, v. 263, no. 5144, p. 198–200, doi:10.1126/Science.263.5144.198 (in Articles).

Hall, D.K., and Riggs, G.A., 2007, Accuracy assessment of the MODIS snow products: Hydrological Processes, v. 21, p. 1534–1547.

Hall, D.K., Foster, J.L., and Chang, A.T.C., 1982, Measurement and modeling of microwave emission from forested snowfields in Michigan: Nordic Hydrology, v. 13, no. 3, p. 129–138.

Hall, D.K., Chang, A.T.C., Foster, J.L., Benson, C.S., and Kovalick, W.M., 1989, Comparison of in situ and Landsat derived reflectance of Alaskan glaciers: Remote Sensing of Environment, v. 28, no. 1, p. 23–31.

Hall, D.K., Riggs, G.A., Salomonson, V.V., DiGirolamo, N.E., and Bayr, K.I., 2002, MODIS snow-cover products: Remote Sensing of Environment, v. 83, nos. 1–2, p. 181–194.

Hall, D.K., Foster, J.L., Robinson, D.A., and Riggs, G.A., 2004, Merging the MODIS and RUCL monthly snow-cover records, in Proceedings, International Geoscience and Remote Sensing Symposium 2004, Anchorage, Alaska, 20–24 September 2004: p. 1318–1321.

Hall, D.K., Key, J.R., Casey, K.A., Riggs, G.A., and Cavalieri, D.J., 2004, Sea ice surface temperature product from MODIS: Institute of Electrical and Electronic Engineers Transactions on Geoscience and Remote Sensing, v. 42, no. 5, p. 1076–1087.

Hallikainen, M.T., 1984, Retrieval of snow water equivalent from Nimbus-7 SMMR data—Effect of land-cover categories and weather conditions: Institute of Electrical and Electronic Engineers, Journal of Oceanic Engineering, v. OE–9, no. 5, p. 372–376.

Hoyos-Patiño, Fabian, 1998, Glaciers of Colombia, *in* Williams, R.S., Jr. and Ferrigno, J.G., eds., Satellite image atlas of glaciers of the world: U.S. Geological Survey Professional Paper 1386–I (Glaciers of South America), p. I111–I130. [*http://pubs.usgs.gov/pp/p1386i*]

Hughes, M.G., and Robinson, D.A., 1996, Historical snow cover variability in the Great Plains region of the USA—1910 through to 1993: International Journal of Climatology, v. 16, no. 9, p. 1005–1018.

Hughes, M.G., Frei, A., and Robinson, D.A., 1996, Historical analysis of North American snow cover extent—Merging satellite and station derived snow cover observations, in Proceedings, 53d Eastern Snow Conference, Williamsburg, Va., 1–3 May 1996, p. 21–32.

Kelly, R.E.; Chang, A.T.; Tsang, Leung; and Foster, J.L., 2003, A prototype AMSR-E global snow area and snow depth algorithm: Institute of Electrical and Electronic Engineers, Transactions on Geoscience and Remote Sensing, v. 41, no. 2, p. 230–242.

Kelly, R.E.J., Chang, A.T.C., and Foster, J.L., 2004, [updated daily], AMSR-E/Aqua daily L3 global snow water equivalent EASE-Grids V001, March to June 2004, Boulder, Colo., USA: National Snow and Ice Data Center, digital data. [nsidc.org/data/docs/daac/ae_swe_ease-grids.gd.html]

Kelly, R.E.J., Chang, A.T.C., Foster, J.L., and Hall, D.K., 2004, Using remote sensing and spatial models to monitor snow depth and snow water equivalent, *in* Kelly, R.E.J., Drake, N.A., and Barr, S.L,. eds., Spatial modelling of the terrestrial environment: Chichester, West Sussex, England; Hoboken, N.J., p. 35–58.

Kidwell, K.B., 1998, Polar stereographic Earth location App. A of NOAA Polar Orbiter data user's guide: Suitland, Md., U.S. Department of Commerce. [*http://www2.ncdc.noaa.gov/docs/podug/html/a/app-a.htm*]

Klein, A.G., and Stroeve, Julienne, 2002, Development and validation of a snow albedo algorithm for the MODIS instrument: Annals of Glaciology, v. 34, p. 45–52.

Klein, A., and Barnett, A.C., 2003, Validation of daily MODIS snow maps of the Upper Rio Grande River Basin for the 2000–2001 snow year: Remote Sensing of Environment, v. 86, no. 2, p. 162–176.

Knap, W.H., Reijmer, C.H., and Oerlemans, J., 1998, Narrowband to broadband conversion of Landsat TM glacier albedos: International Journal of Remote Sensing, v. 20, no. 10, p. 2091–2110.

Kukla, George, 1981, Climatic role of snow covers, *in* Allison, Ian, ed., Sea level, ice, and climate change: International Association of Hydrological Sciences, IAHS Publication no. 131, Wallingford, Oxforshire OX10 8BB, England, U.K., p.79–107.

Kukla, George, and Robinson, David A., 1980, Annual cycle of surface albedo: Monthly Weather Review, v. 108, no. 1, p. 56–68.

Kukla, George, and Robinson, David A., 1981, Accuracy of operational snow and ice charts: 1981 Institute of Electrical and Electronic Engineers, International Geoscience and Remote Sensing Symposium, Digest, p. 974–987.

Kunzi, K.F., Patil, S., and Rott, H., 1982, Snow-cover parameters retrieved from Nimbus-7 Scanning Multichannel Microwave Radiometer (SMMR) data: Institute of Electrical and Electronic Engineers, Transactions on Geoscience and Remote Sensing, v. GE–20, no. 4, p. 452–467.

Matson, M., Roeplewski, C.F., and Varnadore, M.S., 1986, An atlas of satellite-derived Northern Hemisphere snow cover frequency: Washington, D.C., National Weather Service, 75 p.

Mätzler, Christian, and Schanda, Erwin, 1984, Snow mapping with active microwave sensors: International Journal of Remote Sensing, v. 5, no. 2, p. 409–422.

McFadden, J.D., and Ragotzkie, R.A., 1967, Climatological significance of albedo in central Canada: Journal of Geophysical Research, v. 72, no. 4, p. 1135–1143.

Mekler, Yuri, and Joseph, J.H., 1983, Direct determination of surface albedos from satellite imagery: Journal of Climate and Applied Meteorology, v. 22, no. 4, p. 530–536.

Mellor, M., 1964, Snow and ice on the Earth's surface, U.S. Army Corps of Engineers, Cold Regions Research and Engineering Laboratory, Research Report 11–C1, 163 p.

Meteorological Service of New Zealand, n.d., Information Publication No. 15. [*http://www.metservice.co.nz/default/index.php?pkey=190512&class=menu*]

Morales Arnao, Benjamín, and Hastenrath, S.L., 1998, Glaciers of Perú, *in* Williams, R.S., Jr., and Ferrigno, J.G., eds., Satellite image atlas of glaciers of the world: U.S. Geological Survey Professional Paper 1386–I (Glaciers of South America), p. I151–I179. [*http://pubs.usgs.gov/pp/p1386i*]

National Academy of Sciences, 2004, Climate data records from environmental satellites—Interim report: Washington, D.C., National Academy Press, 136 p.

Nghiem, S.V., and Tsai, W.-Y., 2001, Global snow cover monitoring with spaceborne K-band scatterometer: Institute of Electrical and Electronic Engineers, Transactions on Geoscience and Remote Sensing, v. 39, no. 10, p. 2118–2134.

Nolin, A.W., and Liang, S., 2000, Progress in bidirectional reflectance modeling and applications for surface particulate media—Snow and soils: Remote Sensing Reviews, v. 18, no. 2, p. 307–342.

Nolin, A.W., Dozier, J., and Mertes, L.A.K., 1993, Mapping alpine snow using a spectral mixture modeling technique: Annals of Glaciology, v. 17, p. 121–124.

Papa, Fabrice; Legresy, Benoît; Mognard, N.M.; Josberger, E.G.; and Remy, Frédérique, 2002, Estimating terrestrial snow depth with the TOPEX-POSEIDON altimeter and radiometer: Institute of Electrical and Electronic Engineers, Transactions on Geoscience and Remote Sensing, v. 40, no. 10, p. 2162–2169.

Potts, H.L., 1937, A photographic snow survey method of forecasting from photographs: Transactions, American Geophysical Union, South Continental Divide Snow Survey Conference, p. 658–660.

Ramsay, B.H., 1998, The interactive multisensor snow and ice mapping system: Hydrological Processes, v. 12, nos. 10–11, p. 1537–1546.

Rango, A., Salomonson, V.V., and Foster, J.L., 1977, Seasonal streamflow estimation in the Himalayan region employing meteorological satellite snow cover observations: Water Resources Research, v. 13, no. 1, p. 109–112.

Riggs, G.A., and Hall, D.K., 2003, Reduction of cloud obscuration in the MODIS snow data product: [published in] Proceedings, 60th Eastern Snow Conference, Sherbrooke, Québec, 4–6 June 2003, p. 205–212.

Riggs, G.A., DiGirolamo, N.E., Hall, D.K., 2005, Comparison of MODIS daily global fractional snow cover maps at 0.5- and 0.25-degree resolutions, in Proceedings, 62d Eastern Snow Conference, Waterloo, Ontario, Canada, 7–10 June 2005, p. 21–27.

Rikhter, G.D., 1960, Geografiia snezhnogo pokrova (Geography of the snow cover): Moscow, Izd-vo Akademii nauk SSSR, 220 p.

Robinson, D.A., 1993a: Monitoring Northern Hemisphere snow cover, in Snow Watch '92—Detection strategies for snow and ice: Boulder, Colo., National Snow and Ice Data Center, Glaciological Data Report, GD–25, p. 1–25.

Robinson, D.A., 1993b, Hemispheric snow cover from satellites: Annals of Glaciology, v. 17, p. 367–371.

Robinson, D.A., and Dewey, K.F., 1990, Recent secular variations in the extent of northern hemisphere snow cover: Geophysical Research Letters, v. 17, no. 10, p. 1557–1560.

Robinson, D.A., and Frei, Allan, 2000, Seasonal variability of northern hemisphere snow extent using visible satellite data: Professional Geographer, v. 52, no. 2, p. 307–315.

Robinson, D.A., and Kukla, George, 1985, Maximum surface albedo of seasonally snow-covered lands in the Northern Hemisphere: Journal of Climate and Applied Meteorology, v. 24, no. 5, p. 402–411.

Robinson, D.A., Scharfen, G., Serreze, M.C., Kukla, G., and Barry, R.G., 1986, Snow melt and surface albedo in the Arctic Basin: Geophysical Research Letters, v. 13, no. 9, p. 945–948.

Robinson, D.A., Dewey K.F., and Heim, R.R., Jr., 1993, Global snow cover monitoring—An update: Bulletin of the American Meteorological Society, v. 74, no. 9, p. 1689–1696.

Robinson, D.A., Bamzai, A., and Ramsay, B., 2001, Evaluating Northern Hemisphere snow cover during the satellite era—Variations in extent and associations with temperature: Proceedings, 12th Symposium on Global Change and Climate Variations, Albuquerque, N.M., 14–18 January 2001, p. 36–39.

Robock, Alan, 1980, The seasonal cycle of snow cover, sea ice and surface albedo: Monthly Weather Review, v. 108, no. 3, p. 267–285.

Romanov, P., and Tarpley, D., 2003, Automated monitoring of snow cover over South America using GOES Imager data: International Journal of Remote Sensing, v. 24, no. 5, p. 1119–1125.

Rosenthal, Walter, and Dozier, Jeff, 1996, Automated mapping of montaine snow cover at subpixel resolution from the Landsat Thematic Mapper: Water Resources Research, v. 32, no. 1, p. 115–130.

Rott, H., 1984, The analysis of backscattering properties from SAR data of mountain regions: Institute of Electrical and Electronic Engineers, Journal of Oceanic Engineering, v. 9, no. 5, p. 347–355.

Salomonson, V.V., and Marlatt, W.E., 1968, Anisotropic solar reflectance over white sand, snow and stratus clouds: Journal of Applied Meteorology, v. 7, no. 3, p. 475–483.

Santeford, H.S., 1974, A challenge in snow and ice, *in* Santeford, H.S., and Smith, J.L., eds., Advanced concepts and techniques in the study of snow and ice resources—A United States contribution to the International Hydrological Decade: Washington, D.C., National Academy of Sciences, p. 3–8.

Schaefer, Kevin; Denning, A.S.; and Leonard, Owen, 2004, The winter Arctic Oscillation and the timing of snowmelt in Europe: Geophysical Research Letters, v. 31, no. 22, p. L22205, doi:10.1029/2004GL021035.

Scharfen, G., Barry, R.G., Robinson, D.A., Kukla, G., and Serreze, M.C., 1987, Large-scale patterns of snow melt on Arctic sea ice mapped from meteorological satellite imagery: Annals of Glaciology, v. 9, p. 1–6.

Serreze, M.C., Walsh, J.E., Chapin, F.S., III, Osterkamp, T., Dyurgerov, M., Romanovsky, V., Oechel, W.C., Morison, J., Zhang, T., and Barry, R.G., 2000, Observational evidence of recent change in the northern high-latitude environment: Climatic Change, v. 46, nos. 1–2, p. 159–207.

Simic, A., Fernandes, R., Brown, R., Romanov, P., and Park, W., 2004, Validation of VEGETATION, MODIS, and GOES+SSM/I snow-cover products over Canada based on surface snow depth observations: Hydrological Processes, v. 18, no. 6, p. 1089–1104.

Singer, S.F., and Popham, R.W., 1963, Non-meteorological observations from weather satellites: Astronautics and Aerospace Engineering, v. 1, no. 3, p. 89–92.

Smart, W.M., and Green, R.M., 1977, Textbook on spherical astronomy (6th ed.): New York, Cambridge University Press, 431 p.

Stafford, H.M., 1959, History of snow surveying in the West, in Proceedings of the 27th Annual Meeting of the Western Snow Conference, Portland, Oreg., April 1959, p. 1–12.

Steffen, K., 1987, Bidirectional reflectance of snow at 500–600 nm, *in* Goodison, B.E, Barry, R.G., and Dozier, J., eds., Large-scale effects of seasonal snow cover: International Association of Hydrological Sciences Publication 166, p. 415–425.

Stiles, W.H., and Ulaby, F.T., 1980, The active and passive microwave response to snow parameters–1. Wetness: Journal of Geophysical Research, v. 85, no. C2, p. 1037–1044.

Stiles, W.H., Ulaby, F.T., and Rango, A., 1981, Microwave measurements of snowpack properties: Nordic Hydrology, v. 12, no. 3, p. 143–166.

Stone, R.S., Dutton, E.G., Harris, J.M., and Longenecker, David, 2002, Earlier spring snowmelt in northern Alaska as an indicator of climate change: Journal of Geophysical Research, v. 107, no. D10, p. 4,089, doi: 10/1029/2000JD00286, 2002.

Stroeve, Julienne, Box, J.E., Gao, Feno, Shunlin, Liang, Nolin, Anne, and Schaaf, Crystal, 2005, Accuracy assessment of the MODIS 16-day albedo product for snow—Comparisons with Greenland in situ measurements: Remote Sensing of Environment, v. 94, no. 1, p. 46–60.

Sturm, Matthew, Holmgren, Jon, and Liston, G.E., 1995, A seasonal snow cover classification system for local to global applications: Journal of Climate, v. 8, no. 5, p. 1261–1283.

Thompson, L.G., Mosley-Thompson, Ellen, Davis, M.E., Henderson, K.A., Brecher, H.H., Zagorodnov, V.S., Mashiotta, T.A., Lin, P.-N., Mikhalenko, V.N., Hardy, D.R., and Beer, Jürg, 2002, Kilimanjaro ice core records—Evidence of Holocene climate change in tropical Africa: Science, v. 298, no. 5593, p. 589–593, doi:10/1126/Science.1073198 (in Reports).

Ulaby, F.T., and Stiles, W.H. , 1981, Microwave response of snow: Advances in Space Research, v. 1, no. 10, p. 131–149.

Ulaby, F.T., Moore, R.K., and Fung, A.K., 1986, Microwave remote sensing, active and passive—V. 3, From theory to applications: Reading, Mass., Addison-Wesley, 2,162 p.

Vernekar, A.D., Zhou, J., and Shukla, J., 1995, The effect of Eurasian snow cover on the Indian monsoon: Journal of Climate, v. 8, no. 2, p. 248–266.

Waite, W.P., and McDonald, H.C., 1970, Snowfield mapping with K-band radar: Remote Sensing of Environment, v. 1, no. 2, p. 143–150.

Walker, A.E., and Goodison, B.E., 1993, Discrimination of a wet snow cover using passive microwave satellite data: Annals of Glaciology, v. 17, p. 307–311.

Walsh, J.E., 1984, Snow cover and atmospheric variability: American Scientist, v. 72, no. 1, p. 50–57.

Whetton, P.H., Haylock, M.R., and Galloway, R., 1996, Climate change and snow-cover duration in the Australian Alps: Climatic Change, v. 32, no. 4, p. 447–479.

Williams, R.S., Jr., and Ferrigno, J.G., eds., 1998, Glaciers of South America: U.S. Geological Survey Professional Paper 1386–I, 206 p. [*http://pubs.usgs.gov/pp/p1386i*]

Winther, J.-G., Gerland, S., Ørbæk, J.B., Ivanov, B., Blanco, A., and Boike, J., 1999, Spectral reflectance of melting snow in a high Arctic watershed on Svalbard—Some implications for optical satellite remote sensing studies: Hydrological Processes, v. 13, nos. 12–13, p. 2033–2049.

Young, J.A.T., and Hastenrath, Stefan, 1991, Glaciers of Africa, *in* Williams, R.S., Jr., and Ferrigno, J.G., eds., Satellite image atlas of glaciers of the world: U.S. Geological Survey Professional Paper 1386–G (Glaciers of the Middle East and Africa), p. G49–G70. [*http://pubs.usgs.gov/pp/p1386g*]